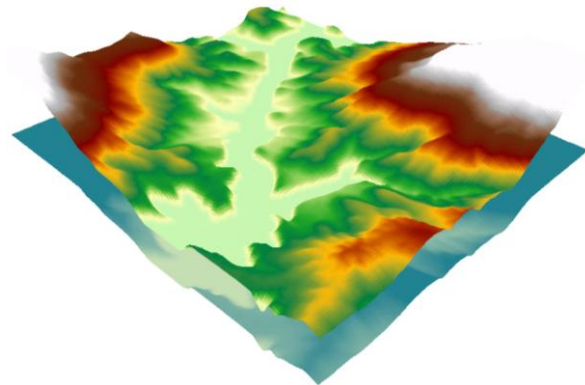


Adama Science and Technology University



Research Final Report

# **Numerical Groundwater Flow Modelling for Slope Stability Analysis: Case of Blue Nile Gorge, Central Ethiopia**



Bisrat Ayalew  
Fasika Mekonen

January 2018

## **ABSTRACT**

*Despite the vast researches on the landslide problem in the Blue Nile Basin, little is known about the perspective of groundwater level fluctuation in the region. The overall image that emerges from literatures is as it upswings in the rainy season from high infiltration into the ground and cause landslide problem. This assumption sustained more than nearly a century in all researches conducted towards understanding the landslide hazard, which causes life-threatening impact besides the negative economic effects to repair structures. Even though different mitigation measures are taken from these studies output and recommendation, the region is still unstable. Accordingly, there is a need for investigation of groundwater flow coupled with slope stability study. In this study, we determined the overall condition of groundwater in different seasons and checked the contribution of the level rise to instability of a slope in a specific site. After an exhaustive site visit and data study, the area is conceptualized based on a geographical, hydrological, and hydrogeological feature of the region, to fit the mathematical model in hand. The groundwater flow study is conducted with identified boundary conditions using saturated finite-difference grid model MODFLOW. Steady and transient states of flow are modelled with different hydrogeological parameters. The models are calibrated to satisfy the observed field conditions and expected results from the scientific point of view. Results show that in limited areas the fluctuation of groundwater is significant while in others the level remains stable in all seasons of the year. Following that, the result of groundwater flow model is exported to GeoStudio to simulate the slope stability of the selected slope. The factor of safety was calculated using slope/W. The effect of pore-water on the factor of safety is crosschecked by remodelling the slope without water. The results and sensitivity analysis of slope stability confirm that the rise of groundwater level decreases the factor of safety significantly only on critical slope section. From this paper, it is noticeable that in landslide study, coupling groundwater model with slope stability is not only effective but also economical in shallow groundwater sites before infrastructure development.*

*Keywords: Blue Nile Gorge, Groundwater Level, MODFLOW, Landslide, slope/W,*

## **ACKNOWLEDGMENTS**

Adama Science and Technology University supported this study. The authors, however, would like to appreciate the contributions made by the Ethiopian Road Authority, Geological Survey of Ethiopia, and National Metrological Agency for the secondary and preliminary data.

## Table of Contents

<i>ABSTRACT</i> .....	i
ACKNOWLEDGMENTS.....	ii
List of Figures .....	iv
List of Tables .....	v
1. Introduction .....	1
1.1. Statement of the Problem.....	3
1.2. Objective of the Study.....	4
1.3. Features of the Study Area.....	4
1.4. Structure of the Report.....	9
2. Literature Review .....	10
3. Materials and Methods.....	13
3.1 Groundwater Flow Modelling.....	13
3.1.1 Spatial Discretization .....	14
3.1.2 Boundary Conditions, Model Parameters, and Stresses.....	15
3.2 Slope Stability Modelling .....	19
4. Results and Discussion .....	21
4.1 Steady State Model Development and Simulation.....	21
4.2 Transient Model Development and Simulation .....	22
4.3 Slope Stability Analysis .....	26
5. Model Calibration .....	31
6. Conclusion and Recommendation .....	37
7. References .....	39
Appendix .....	42

## List of Figures

Figure 1 Location of the Study area (a), Major River of Ethiopia (boundaries from Ministry of Water and Electricity) (b) .....	5
Figure 2 Schematic geological sections and regions in the BNG along the road (Ayalew L and Yamagishi H, 2003) with few adjustments and changes .....	6
Figure 3 Monthly rainfall at the five selected stations and Thiessen polygons .....	7
Figure 4 Average daily rainfall (mm) over a period from 1994 to 2015 presented monthly .....	8
Figure 5 Average Potential Evapotranspiration of BNG over a period of 2012 to 2015.....	8
Figure 6 Systematics of the workflow .....	13
Figure 7 Top and bottom layers of the Aquifer (left to right).....	16
Figure 8 location of observation wells and springs, model boundaries .....	16
Figure 9 Geological zones used for hydraulic conductivity estimation.....	18
Figure 10 Average historical groundwater level below the earth surface(data from ERA over a period of 2012 to 2015).....	19
Figure 11 Landslide hazard zonation map of BNG (Shiferaw A, 2014) .....	20
Figure 12 Simulated groundwater level at steady state .....	21
Figure 13 Recharge zones (not to scale) and values in m/day .....	22
Figure 14 Contour of computed groundwater level at steady state .....	23
Figure 15 Contour of groundwater level at transient state for month of August (Stress period 8, time step 15).....	24
Figure 16 Simulated groundwater level at transient state.....	25
Figure 17 Gridded Slope geometry, material used and position of pore-water pressure line in the specific slope.....	26
Figure 18 Time trend of rainfall groundwater level and landslide at selected very high landslide zone of the region (Filiklik rainfall station and Pizo-metre B05-13).....	27
Figure 19 Slope stability analysis results (on the left slope analysis with no pore-water pressure and on the right with pore-water pressure imported from MODFLOW at steady state).....	29
Figure 20 Pore-water Pressure and strength along the slope .....	29
Figure 21 Impact of groundwater level rise on FS of the slope.....	30
Figure 22 Measured head versus observed head at steady state .....	32
Figure 23 Hydraulic conductivity of the area after calibration.....	33
Figure 24 Measured head versus observed head at transient state.....	33

## List of Tables

Table 1 Average areal daily rainfall of the study area (2012 to 2015).....	7
Table 2 Available Groundwater level monitoring wells and average groundwater level record in the area over the period of 2012 to 2015 .....	17
Table 3 Hydro-Mechanical Parameters.....	27
Table 4 Water budget of the model at steady state flow simulation .....	35
Table 5 Water budget of the model at transient state of flow .....	36

## **1. Introduction**

Regardless of improvements in science and technology in prediction and mitigating measures, landslides are still exact an economic and environmental toll in mountainous regions of Ethiopia. These hazards are becoming serious concerns to the public and to the planners and decision makers at various levels of the government. However, so far, little efforts have been made to reduce losses from such hazards (Woldearegay, 2013). This is partly due to the complexity of the processes driving slope failures and our inadequate knowledge of the underlying mechanisms. Vast numbers of factors have been investigated in the understanding of the driving force of landslides in the country much more in the Blue Nile Gorge (BNG). According to Woldearegay (2013), even though, many factors contribute to slope failure most of the stability problems in the country are from rainfall infiltration: Earthquake-triggered landslides are little reported.

The BNG, along Gohatsion–Dejen road, is one of the common areas in the country where most slope instabilities are frequently observed. In this road area, it is very common to see slope failure events that hinder traffic movements during the rainy season (Woldegiorgis H, 2008, and Meten M et al, 2015). Huge columnar jointed basalt, groundwater, uncontrolled surface runoff, joints of rocks, and the presence of marl and shale within hard rocks are the main causes of slope instability. During the past years, landslides and rock fall had damaged the road sections, bridges, and farmlands (Woldegiorgis H, 2008). There are still active landslides in the area (Henok Woldegiorgis, 2014)

Many studies conducted in the area to investigate the problem. The recent studies by Japan International Cooperation Agency (JiCA) and Geological Survey of Ethiopia (GSE) identified landslide areas in the region are in continuous movement. Some of these are up to two kilometers wide, putting into jeopardy this vital link (Geo-hazard Investigation Directorate, 2016). Most of the land features in which the road passes through are mountainous, unstable, and highly susceptible to sliding. Even though many kinds of literature conclude, major triggering factor for slope instability in this landscape is groundwater level increase from infiltration into the soil, there is no comprehensive groundwater study in the area, except the above-mentioned field investigation for the purpose of the road protection by JiCA. Nearly all researchers tried to see the failure from

the landscape and geological perspective. Nevertheless, in such landscape groundwater flow is a determinant factor on deferent phenomena including landslide.

Groundwater flow system is dynamically linked to the hydrological cycle through various natural or artificial recharge processes. As part of the hydrological cycle, groundwater is always in motion from regions of recharge to discharge points. Landslide areas are the site of local groundwater storage and moisture retention in an area that would otherwise lose water rapidly to adjacent valley owing to high slope. Because materials offer granular porosity the landslides bodies hold import amount of groundwater, which discharges mostly as diffuse flow or as focused discharge to springs. Typical examples of association of landslides with springs are those occurring in the BNG (Kebede, S., 2012).

Moreover, it is well known that water is one of the major triggers of landslides usually in uplands. Plentiful landslide studies had done so far all over the world. Most of these researchers discuss different effects that water may have on slope stability such as decreasing suction, rising groundwater table and subsequent increase in pore-water pressure, seepage erosion, hydraulic uplift pressure from below the landslide, and influence of water on the plasticity of the landslide. Moreover, researchers point out that long-term rainfall pattern changes have a substantial impact on slope stability. An overall decrease in precipitation results in a lowering of the water table, as well as a decrease in the weight of the soil mass. On the other hand, an increase in precipitation will raise the level of the groundwater, reduce shear strength, increase the weight of the soil mass, and may increase erosion.

Nowadays the advancement of computer technology and applications make models powerful tools for environmental protection: maintaining the groundwater equilibrium system, controlling groundwater level fluctuation, and protecting against severe land subsidence (ASTM, 2010). A model is a representation of a real system or process (Konikow, L. F., and Mercer, J. W., 1988). There are different kinds of models, such as conceptual model, numerical or analytical model, and physical model. A conceptual model is a hypothesis for how a system or process operates a qualitative description of a system and its representation relevant to the intended use of the model. A mathematical model is a representation of a conceptual model with objects, forces, and events replaced with mathematical expressions. A majority of the mathematical models used today to

simulate water flow in both saturated and variably saturated systems are deterministic. Mathematical models generally solve a set of partial differential equations representing conservation of mass, momentum, and energy. Most models use various numerical techniques to solve the governing equations subject to appropriate initial and boundary conditions. Implementation of a numerical algorithm that solves the governing equations results in a computer code that can be considered a generic model.

Even though numerical methods are tools that can aid in studying groundwater problem and can help to increase our understanding of groundwater systems (Mercer, J. W., and Faust, C. R., 1980), they are not simple with reference to computation and need more information about boundary conditions and material properties. As a result, numerical methods are more complicated and their application needs more time and data. Nevertheless, numerical methods provide more accurate results compared to analytical methods ( Surinaidu L. et al, 2015).

The purpose of this study is to characterize groundwater level fluctuations in specific, previously instrumented landslides and adjacent slopes. Firstly, modelling of groundwater flow will be done and the results will be exported to slope stability model in order to identify the status of the selected slope. To do that a comprehensive study of hydrogeological conditions of the site is required. From this work, it is expected to make thorough understanding and conclusion of groundwater level-rainfall-landslide relationships.

### **1.1. Statement of the Problem**

Landslide problems are the less tackled but by far the most disastrous natural hazards in the Blue Nile Gorge in general and in the Dejen-Gohatsion portion in particular. In 1960, a landslide killed 45 people at Gembichi village in the Bechet River valley and in September 1993, another landslide incidence killed an ox and damaged a huge area of agricultural land thereby destroying most of the crops which resulted in food crisis for the livelihood of 700 households (Matebie Meten, 2014). In addition to that, there is a yearly traffic problem in this area after the rainy season due to the damage on the road by rainfall induce landslide.

Many researchers studied landslide and landslide triggering factors in Ethiopia. But, most of them investigated in the geological and landscape factors for slope instability of different areas. Among

the research works conducted in Blue Nile Gorge are “Slope failures in the Blue Nile basin, as seen from landscape evolution perspective” by (H, 2004) and Factors affecting slope stability in the Blue Nile basin by (Ayalew L. , 2000) are some of them. These studies did not see the slope stability related to groundwater level fluctuation.

## **1.2. Objective of the Study**

The objective of the study is to model groundwater level, identifying condition of the area and analyzing slope stability in Gohatsion-Dejen Road. Related to this main objective there is a tendency of including the following specific objectives;

- To investigate the existence of near-surface groundwater from past records in the project area
- To investigate and draw the flow path of the groundwater
- To investigate the condition of the area related to land sliding/slope stability and recommending possible solutions

## **1.3. Features of the Study Area**

The study area is located in Blue Nile Basin, which is situated in the Northwestern part of Ethiopian. It is around 189 to 229 km from the capital city of the country, Addis Ababa. Part of economically important main Addis Ababa- Debremarkos-Bahir Dar-Gondar-Metema-Sudan road and the Gondar-Tigray road that connects north central and Northwestern part of the country with the capital of Addis Ababa and port of Sudan crosses this region.

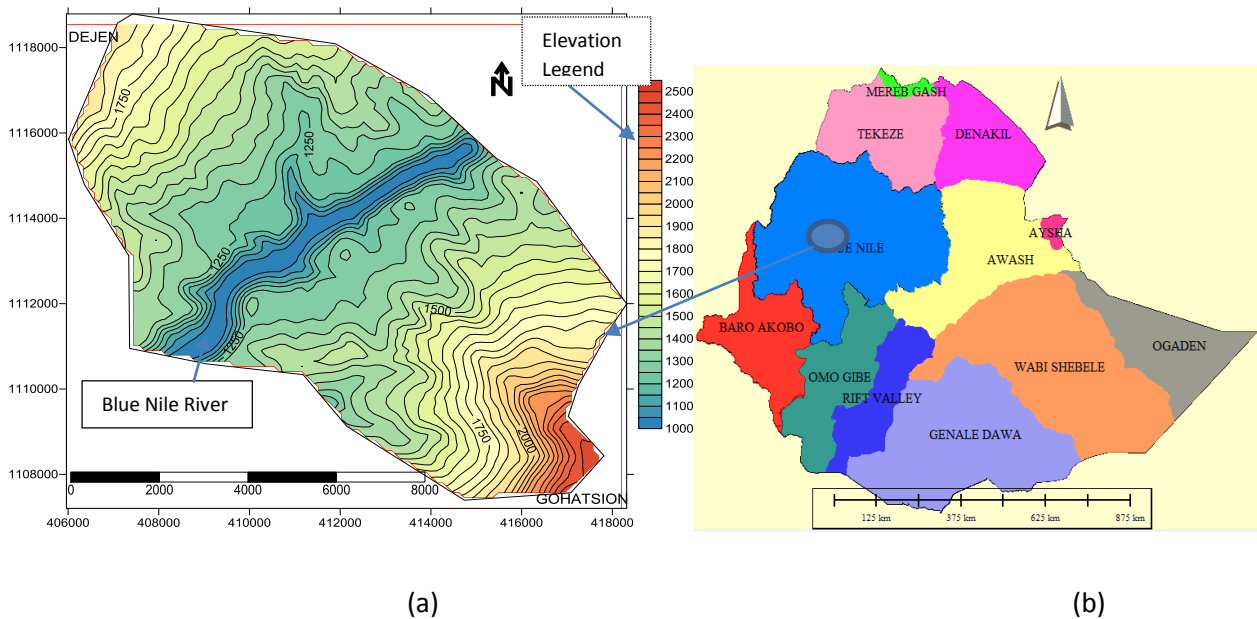


Figure 1 Location of the Study area (a), Major River of Ethiopia (boundaries from Ministry of Water and Electricity) (b)

The BNG landform is that of a basaltic lava plateau (Eocene period flood lava), with an elevation of about 2,500m, underlain by Mesozoic sedimentary rocks of various origin and type as low as 1,028m above mean sea level (Geo-hazard Investigation Directorate, 2016). Lateral slopes of BNG consist of several levels including cliffs and Colluvial slopes. These gentle slopes develop in the areas of limestone and shale, which are covered by residual soil and Colluvial deposits. Although the sedimentary and volcanic rocks in the area are exposed largely as symmetrical stratigraphy on both sides of the Blue Nile River, the detailed sequences are unevenly distributed. The sequence in the area is not disturbed due to major faults and is generally horizontally stratified. Figure 2 shows a schematic geological cross-section of the Nile (Ayalew L and Yamagishi H, 2003). (Ayalew L and Yamagishi H, 2003)

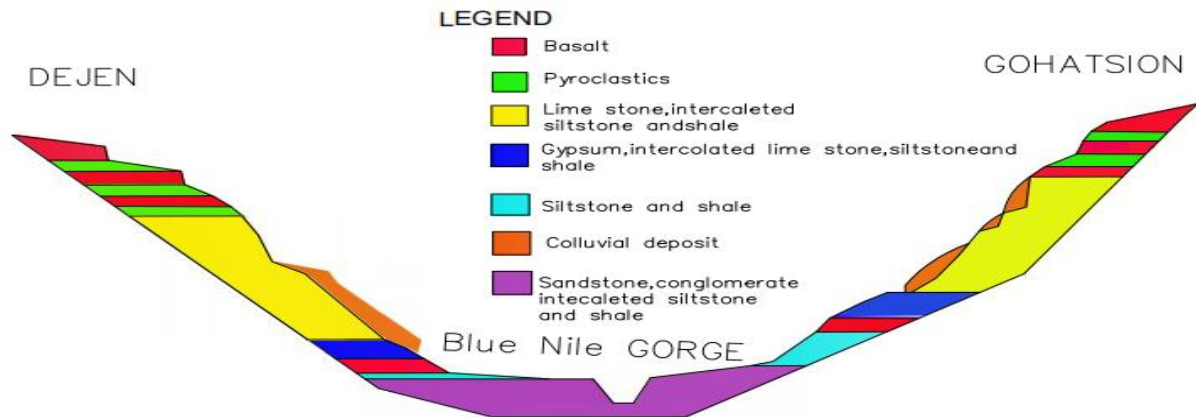


Figure 2 Schematic geological sections and regions in the BNG along the road (Ayalew L and Yamagishi H, 2003) with few adjustments and changes

The climate in BNG is warm and temperate. The average temperature is 19.5 °C with a maximum of 37.7 °C. The rainy season is at the end of May to September, with July and August accounting for approximately half of annual precipitation. The average, minimum and maximum rainfall in the area is 1270, 1209 and 1362 millimeter per year respectively over 22 years record from 1994 to 2015. Figure 4 shows 22 years average monthly rainfall pattern of the area. The precipitation in the region is fairly regular year to year. At the site of interest, there are five rainfall-measuring stations namely Blue Nile Sheleko, Church, Bridge, Filiklik, and Gohatsion. For groundwater recharge from rainfall adjustment, the coverage of the area by each station is approximated by Thiessen polygon method as shown in Figure 3. This result is going to be used later in the adjustment of recharge in groundwater flow analysis. Groundwater recharge in this basin is 100mm to 303mm per year (Asmerom, G. H., 2008).

Table 1 Average areal daily rainfall of the study area (2012 to 2015)

STATIONS	UTM-E(M)	UTM-N (M)	MEAN PPT(MM)	AREA(KM <sup>2</sup> )	PPT*A
Gohatsion	416740.6	1105795	3.32	5.16	17.11932
Filkilik	417045.9	1111289	3.31	22.28	73.7816
Bridge	411243.5	1113902	3.73	41.98	156.6052
Sheleko	407605.1	1117869	3.32	2.66	8.832061
Church	407763.5	1117242	3.71	14.55	53.97588
Total				86.63	310.314
				PPT	3.582062

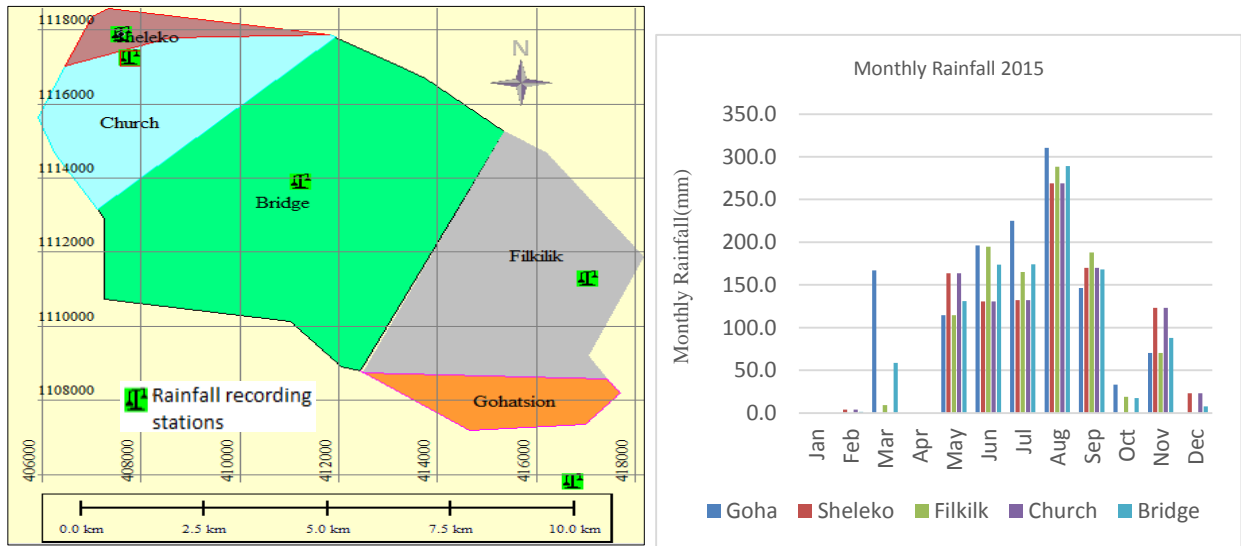


Figure 3 Monthly rainfall at the five selected stations and Thiessen polygons

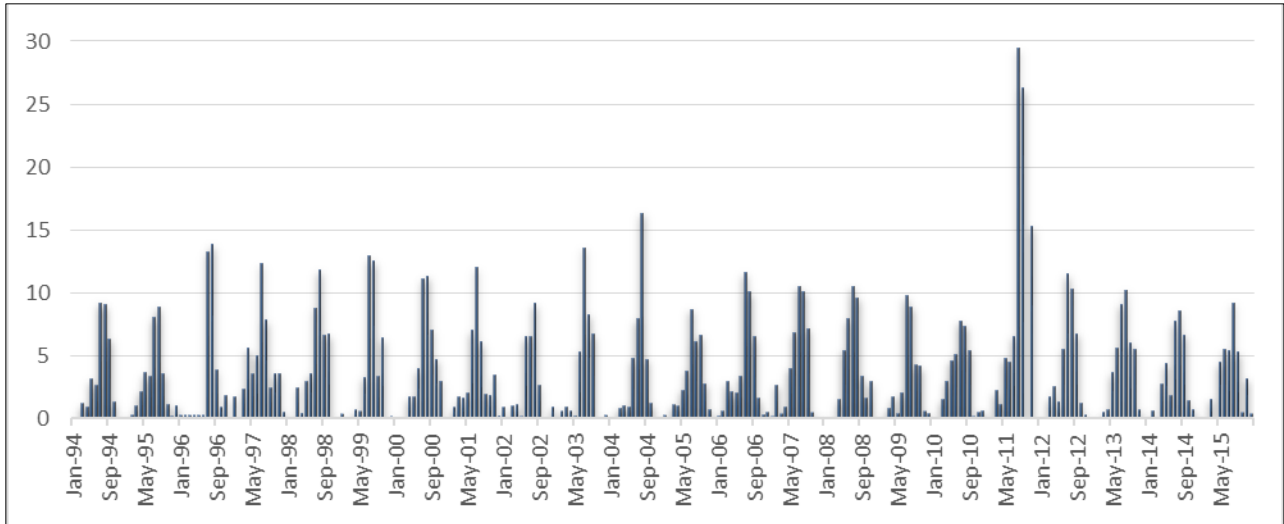


Figure 4 Average daily rainfall (mm) over a period from 1994 to 2015 presented monthly

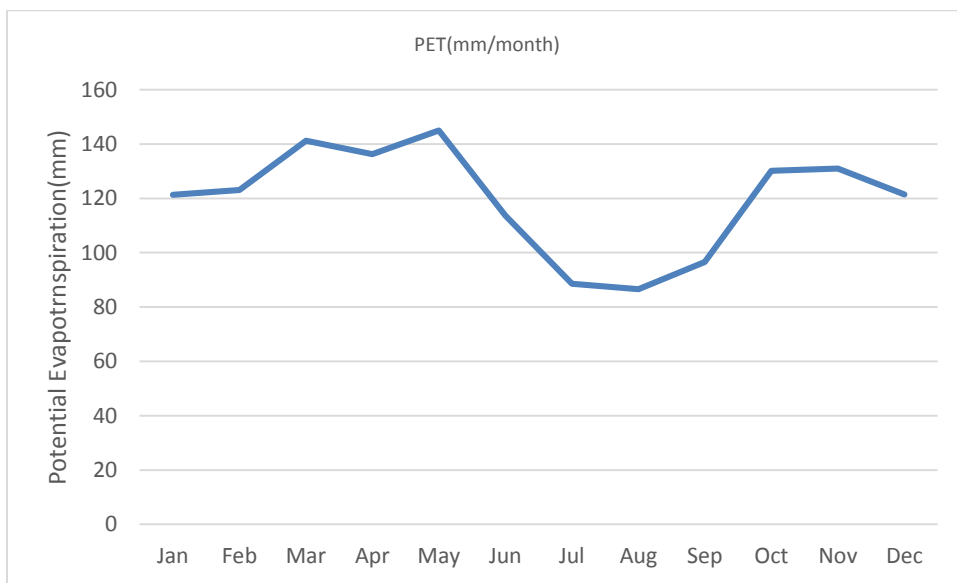


Figure 5 Average Potential Evapotranspiration of BNG over a period of 2012 to 2015

The Blue Nile River crosses this area. It is the largest and perennial river in this site of interest. There are also small streams, which run from the hilly side and dry out after a few periods of the rainfall period. The runoff and recharge in the basin, in general, depend on the topography and rainfall amount. The relatively flat area of the region is dominantly covered with agricultural crops while the hilly area is covered with lightly dispersed small trees.

#### **1.4. Structure of the Report**

This report is organized into six main parts. Part one is an introduction, which deals with the problem of the study area, related to a landslide, the objective, and the mathematical modelling aspect. Part two gives the literature review on past works in the area related to a landslide. It also discusses the problem in the world in general and the scholar works regarding the landslide disaster especially related to groundwater level rise. Part three gives an overview of the method and materials of the research, it includes a description of the systematics of the work, data collection, solution techniques, processing and analysis, groundwater modelling and slope stability modelling. Part four is the result and discussion part of the work. Model calibration is presented in part five of the paper. Part six is about conclusion and recommendation. Finally, in part seven list of the references are presented followed by an appendix.

## 2. Literature Review

The highlands of Ethiopia are generally characterized by highly variable topography, which is a reflection of the past geological and erosion process (Woldearegay, 2013). The landscape includes plateaus, steep hillslopes, and deeply incised valleys and gorges. In addition to the variability and complexity of topography, geology, hydrology, and land use conditions according to Woldearegay (2013), many of the hillslopes are steep enough to reach the limit equilibrium state, whereby external factors such as rainfall infiltration could trigger slope failures. There are some reports that show as the Ethiopian landmass has been frequently affected by first time as well as reactivated old landslides (Saed, 2005).

Landslides in mountainous terrain often occur during or after heavy rainfall, resulting in the loss of life and properties. BNG is among the common landslide areas in the country. In the study area, a landslide occurs almost in every rainy season and was reported by different organizations (Ethiopian Road Authority (ERA), and GSE). Regarding in the area, different researches are done and among these the most recent one are (Ayalew L and Yamagishi H, 2003; Saed, 2005; Woldegiorgis H, 2008; Henok Woldegiorgis, 2014; Shiferaw A, 2014; Meten M et al, 2015; Ayalew, 2009). Most of these studies focus on landslide hazard zonation and mapping. The studies show the complexity of landslide problems in the area.

In BNG, the road damage is a common phenomenon of the mid to end of each rainy season due to the gradual weakening of the soft and weathered rocks by heavy rain and groundwater percolation through big columnar joints of basalt to the underlying limestone formation bearing mudstone and shale at its top and middle strata (Meten M et al, 2015). Such incidences happened due to the progressive softening of weathered basalt and pyroclastic rocks by heavy rainfall, groundwater recharge through the columnar joints of basalt and by a gushing stream, which crosses a road.

Different interdisciplinary researches show that landslides and landslide-generated ground failures are among the common and widespread geoenvironmental hazards in many of the hilly and mountainous terrains of the world (Woldearegay, 2013; Kjekstad, 2009). Due to this, slope instability study is increasingly getting attention in many countries around the world.

The causes of landslides in slopes are attributed to a number of factors. Even though rainfall is a known and the most significant triggering factors for landslides (Ng, 1988), earthquakes, changes in land cover etc are some of the most important landslide triggering factors (Johnson, 1990; Leroueil, 1996; Van Asch, 1999). These hydro-geomorphic events depend on the combination of predisposing factors (e.g. lithology and morphology), triggering factors (e.g. excessive and intense precipitations) and accelerating (e.g. human activities altering natural slope stability) factors along with gravitational forces.

Groundwater level due to rain fills the empty space between seeds of rock and the fractures that are available in them. Such changes in water level can be an effective factor in the stability of the slopes. Another aspect of the influence of water on slopes stability is the pore pressure. The soil in the deep parts of the ground is contained seeds with compact structure, and the pore-water occupies a little space. Due to the high weight of overburden, water can apply a high pore pressure, which led to a reduction in normal effective pressure, and this is a contributing factor to the stability of the slopes and as a result, the shear strength is reduced.

In general, the rainfall infiltration could result in changing the suction and the moisture of soil, raising the unit weight of soil, and reducing the shear strength of soil in the colluvium of the landslide. Increasing pore-water pressure decreases the shear strength of the soil, which may lead to slope failure (Iverson, 2000; van Asch, 2007). The stability of landslide is closely related to the groundwater pressure in response to rainfall infiltration, the geological and topographical conditions, and the physical and mechanical parameters. To assess the potential susceptibility to a landslide, an effective modelling of the rainfall-induced landslide is essential (Tsaparas, 2002; Jiao, 2005).

Extensive human interaction, uncontrolled land use, and enhanced forest clearing increase the susceptibility of surface soil to instability (Sidle, 2006). Furthermore, the actual intensity, frequency, and location of the hazard areas may change over the globe because of changing precipitation patterns and migration due to climate change. More frequent high-intensity rainfall events and higher winter precipitations may increase the risk for landslides.

Accurate slope stability analysis of pre-existing landslides and adjacent, potentially landslide-prone slopes requires a realistic estimation of maximum groundwater levels. Nowadays the researchers are trying to integrate the role of groundwater rise into landslide triggering factors. Groundwater plays a significant role in slow-moving landslides (Hong, 2011). By integrating infiltration-seepage-stability to achieve a coupled time-dependent analysis, the factor of safety of the slope can be computed under various rainfall conditions and pore pressure distributions.

Several studies performed coupled analysis to simulate some actual landslide problems in these years (Gasmo, 2000; Rahardjo, 2001; Corsini, 2006; Calvello, 2008). As we know, hydrogeologic properties are the key components and input to numerical analysis. Landslide triggering mechanisms related to hydrogeology are very complex. This is because on the one hand hydrogeological processes take place in the underground and are hardly accessible. On the other hand, the permeability of the landslide mass, which controls largely the groundwater flow, may be very heterogeneous (Guglielmi, 2002). Preferential flow paths and local formation of coned and perched aquifers complicate the hydrogeology of a landslide (Debieche, 2002). Furthermore, the groundwater flow pattern may change in time because of landslide activity, the formation of cracks and increased permeability due to soil saturation. Because of this complexity, still many uncertainties exist about the hydrological processes occurring in landslides.

### 3. Materials and Methods

The objective of the research achieved via a series of tasks systematically. The necessary data are collected both from organizations and from the site. The collected data include daily rainfall record, hourly groundwater head, and hydrogeological characters of the aquifer, and geomechanical properties. All the data were collected from ERA, Metrological Agency of Ethiopia, and GSE except soil strength properties. These data were examined, organized, and prepared as the form that is acceptable to the software using Microsoft Excel sheet, Surfer, and Global Mapper applications. Following that all data organizations and modelling are done accordingly. Brief systematics of methods followed is depicted in the following figure.

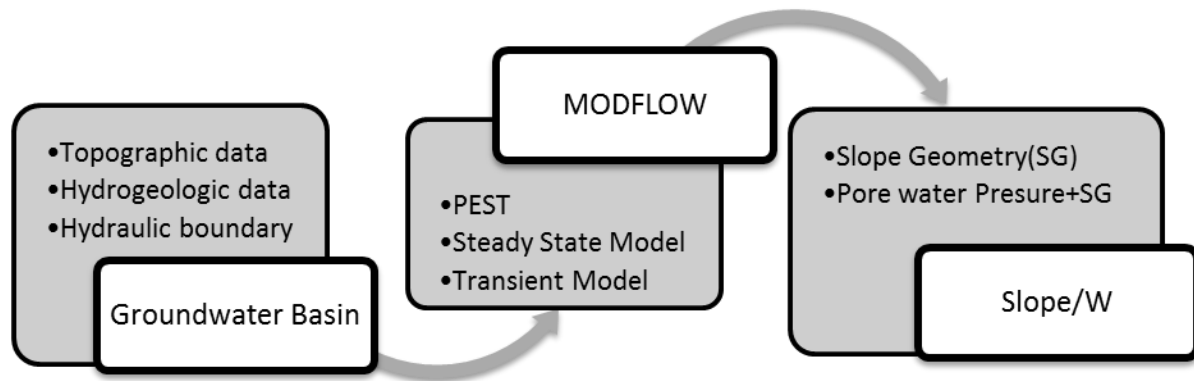


Figure 6 Systematics of the workflow

#### 3.1 Groundwater Flow Modelling

The selection of an appropriate method for modelling a particular problem depends on many factors, such as the number of series to be modelled, required accuracy, modelling costs, ease of use of the models, ease of interpretation of the results ( Mondal, M.S. and Wasimi, S.A, 2006). The numerical finite-difference model (MODFLOW) was used to simulate groundwater flow, a widely used modular three-dimensional block-centred code (Harbaugh, A. W., Banta, E. R., Hill, M. C., and McDonald, M. G., 2000) in Processing MODFLOW modelling environment (Chiang, W. H., and Kinzelbach, W., 1998). Processing MODFLOW is a graphical interface that integrates MODFLOW with various packages to simulate a specific feature of a hydrologic system. It enables representing a wide range of drainage situations, geometry, configurations, and different hydraulic settings. MODFLOW can simulate transient or steady-state saturated groundwater flow in three

dimensions. It offers a variety of boundary conditions, including specified head, areal recharge, evapotranspiration, drains, rivers, and streams (Harbaugh, 2005).

Aquifer units may be confined, unconfined, or treated as convertible between confined and unconfined states. In this extent, non-uniform and the highly variable vertical relationship between the aquifer layers and the overlying confining beds make the assumption of different model layers difficult. Therefore, the region was simulated in steady state and unsteady state, unconfined aquifer, and single layer approach, which is more practical to avoid complications because of many unknown parameters and geometrical condition of multilayer approach.

The basic principle of groundwater flow fundamentally lies in Darcy's law. When this law put together with an equation of continuity, which describes the conservation of fluid mass during flow through a porous medium, can be described by the general flow equation in three dimensions for a heterogeneous anisotropic material. The partial differential equation of groundwater flow used in MODFLOW is (McDonald, 1988)

$$\frac{\partial}{\partial x} \left( K_{xx} \frac{\partial h}{\partial x} \right) + \frac{\partial}{\partial y} \left( K_{yy} \frac{\partial h}{\partial y} \right) + \frac{\partial}{\partial z} \left( K_{zz} \frac{\partial h}{\partial z} \right) \pm W = S_s \frac{\partial h}{\partial t}$$

Where:  $K_{xx}$ ,  $K_{yy}$  and  $K_{zz}$  are values of hydraulic conductivity in the x, y and z directions along Cartesian coordinates Axes, h is hydraulic head, W is volumetric flux per unit volume and represents sink and/or sources,  $S_s$  is the specific storage of the porous material and t is time

The groundwater flow process solves the above equation using the finite-difference method in which the groundwater flow system is divided into a grid of cells. For each cell, there is a single point, called a node, at which head is calculated.

### 3.1.1 Spatial Discretization

Model grids discrete the continuous natural system into cells that allow the numerical solution to be calculated. The spacing between nodes, which is called grid resolution, should be responsive to sharp changes. The overall size of the grid should be adequate to define the problem and the results of the procedure consistent with modelling objectives, but not so large to cause excessive preparation and computation requirements.

The modelled area is replaced by a set of discrete nodes in a grid pattern covering the modelled area. The grid consists of 324 rows and 292 columns overlaying on the 86.431 square kilometers. Furthermore, it is refined around the observation wells in order to increase the calculation precision of the model. Since the aquifer dimension is not rectangular, it shows that the model domain in MODFLOW exceeds the study area defined in the conceptual model. Therefore, we defined the IBOUND by first establishing the lateral extent of the formation using the catchment boundary map and assigned a cell as active if the formation covered more than 50 percent of the cell area.

### 3.1.2 Boundary Conditions, Model Parameters, and Stresses

Following model area discretization, the necessary data for each cell was entered, i.e. top, and bottom of the aquifer, hydraulic conductivity, specific yield coefficient, and porosity of the formation, etc. The input data for the simulation model may be classified as spatial and temporal. The spatial input includes aquifer characteristics, such as water levels, boundaries, hydraulic conductivity, storage coefficient, the location of wells, recharge area, drainage area, etc., whereas the temporal input includes time-dependent data especially for transient modelling.

The boundary condition, grid dimensions, initial aquifer properties, and time steps features are specified as the basic components of the model. The surface topography was derived from a survey carried out over the area and the aquifer extent was structured based on the available details of the boreholes stratigraphic entity. The mean thickness of the unconfined layer was 400 m comprising different hydrogeological fields.

The top of the aquifer layer is assumed on average 12 m below the ground elevation and drawn from the 30m by 30m resolution digital elevation model (DEM). The DEM data is processed to generate grid file to be in a format compatible to the Processing MODFLOW Pro (Version 8.0.15) and imported to the model with elevation referenced according to its geographic position. The imported grid elevation has an elevation range of 1028 to 2500 m. In order to avoid drying of cells during simulations elevated zones were given different thickness based on their depth from the correctional view, relatively higher thickness at higher cells.

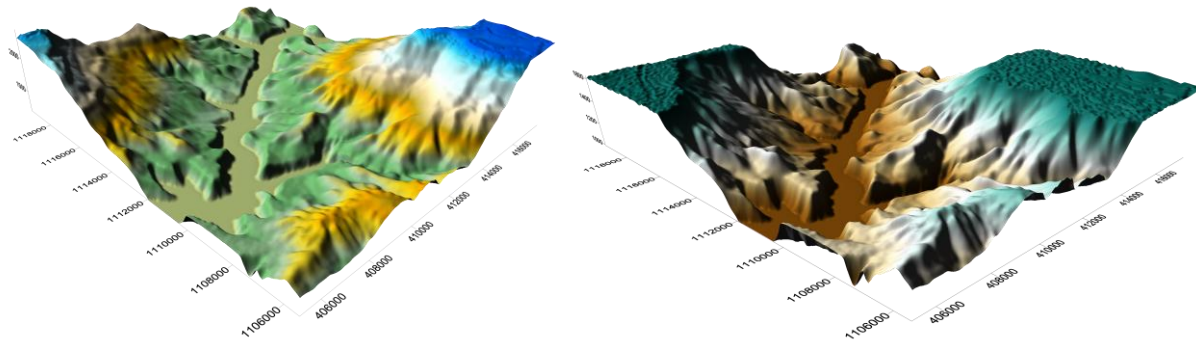


Figure 7 Top and bottom layers of the Aquifer (left to right)

Hydraulic boundary conditions are mathematical statements specifying the dependent variable (head) or the derivative of the dependent variable (flux) at the boundaries of the problem domain. Setting the boundary is the critical step in the modelling and controls the water entrance and exit point of the model system. Three types of boundary conditions were used to define the groundwater flow system in the study area: no-flow boundaries, specified flux boundaries, and constant head boundaries. Geologic or hydrologic barriers to groundwater flow were simulated using no-flow boundaries.

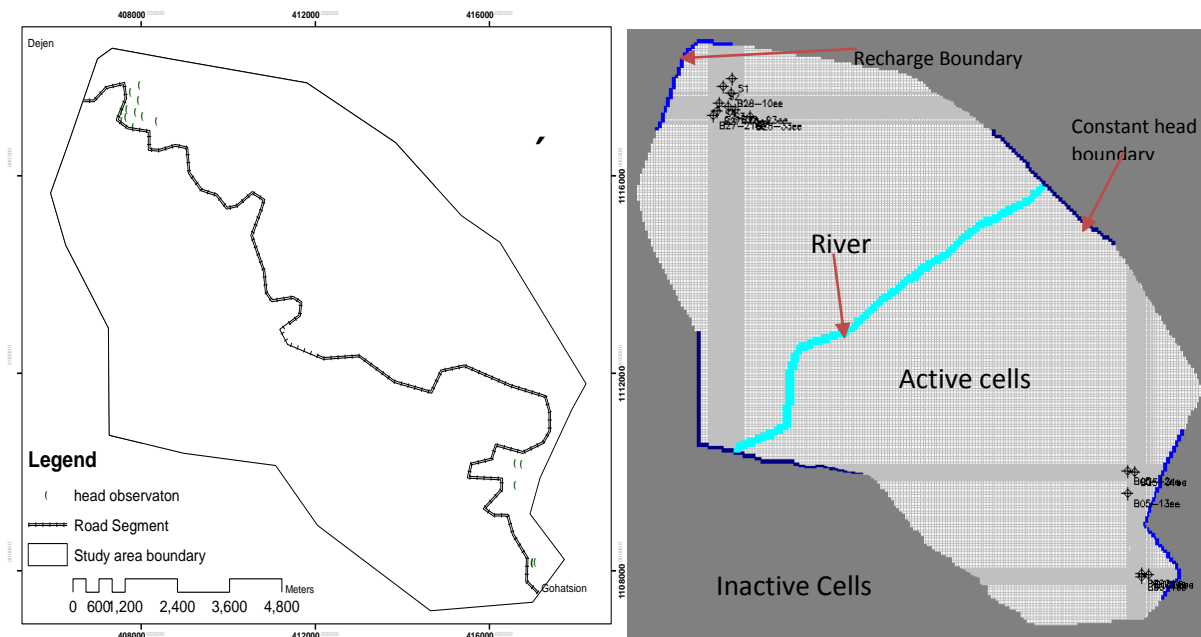


Figure 8 location of observation wells and springs, model boundaries

Table 2 Available Groundwater level monitoring wells and average groundwater level record in the area over the period of 2012 to 2015

UTM-E(M)	UTM-N (M)	LABEL	AVERAGE HEAD
408377.53	1117112.72	B28-33	1623.79
408059.00	1117225.00	B28-23	1687.03
407964.73	1117551.01	B28-10	1716.15
407842.42	1117003.15	B27-24	1682.92
407578.00	1117121.00	B27-21	1727.64
407671.00	1117206.00	B27-10	1723.37
407582.00	1117344.00	B27-09	1756.86
416765.00	1110169.00	B05-31	2113.26
416621.00	1110184.00	B05-12	2079.62
417016.00	1108177.00	B00-21	2369.63
417078.01	1108174.46	B00-16	2398.45
417013.00	1108159.00	B00-14	2370.19
416620.80	1109749.12	B05-13	2222.40

The major perennial river (Blue Nile River) is another important boundary condition, which facilitates the movement of groundwater to and from the river. The flux of water between the groundwater system and rivers is generally dependent on the hydraulic head in the groundwater system and is simulated as a head-dependent flux boundary. Cells in the model that corresponds to the locations of perennial streams are mathematically represented in a manner that allows groundwater to move between the aquifer and stream with a direction and magnitude that depends on the head relations. In order to simulate the interaction of the surface and groundwater, the model used the river package (McDonald, 1988). Estimated riverbed conductance was based on model calibration.

The drain package was used to simulate effects of springs, which remove groundwater from the aquifer at a rate proportional to the head difference between the aquifer and the drain. When the hydraulic head in the aquifer is greater than the drain elevation, groundwater flows into the drain and is removed from the groundwater model.

The very indispensable parameter in the aquifer system is the hydraulic conductivity that defines the flow rate of the groundwater in the aquifer system. Hydraulic conductivity can be defined as the volume of water that will move through a porous medium in unit time under a unit hydraulic

gradient through a unit area measured at right angles to the direction of flow. Hydraulic conductivity is a function of both the medium and the fluid. The model uses the spatial distribution of the hydraulic map described in the conceptual model to begin the model simulation. In this model, groundwater flow within the layer was assumed horizontal.

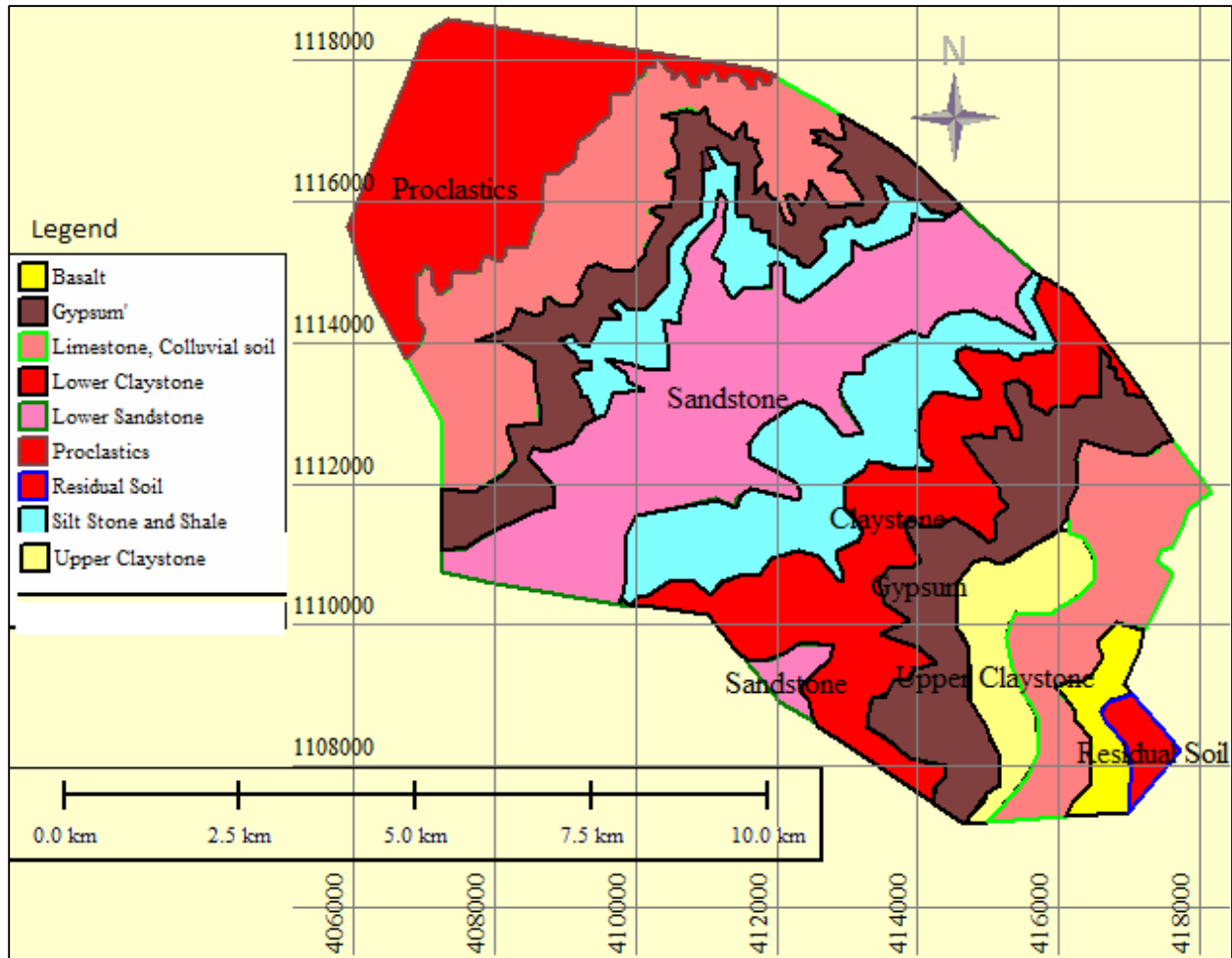


Figure 9 Geological zones used for hydraulic conductivity estimation

Recharge is a specific flux boundary, which is independent of the head of the cell, but MODFLOW consider it as a property for spatially distributed all over the model area. Recharge to the model consisted of infiltration from direct precipitation, stream infiltration draining the Northeast and Southeast escarpments. Recharge was applied to the active model area as a spatially varying, specified flux to the highest active cell. In general, precipitation recharge varies spatially with land surface permeability, which is a function of soil characteristics and land use, and spatial

distribution and intensity of rainfall. For the year period (365 days), different recharges for the five recharge zones (as zoned based on Thieson polygons) as input into the model. The recharge is applied to the model are with recharge package. As it is a boundary property, the recharge has a mathematical code that assumes the volumetric rate of flow into cell described with the multiplication of the recharge rate by the horizontal area of the cell.

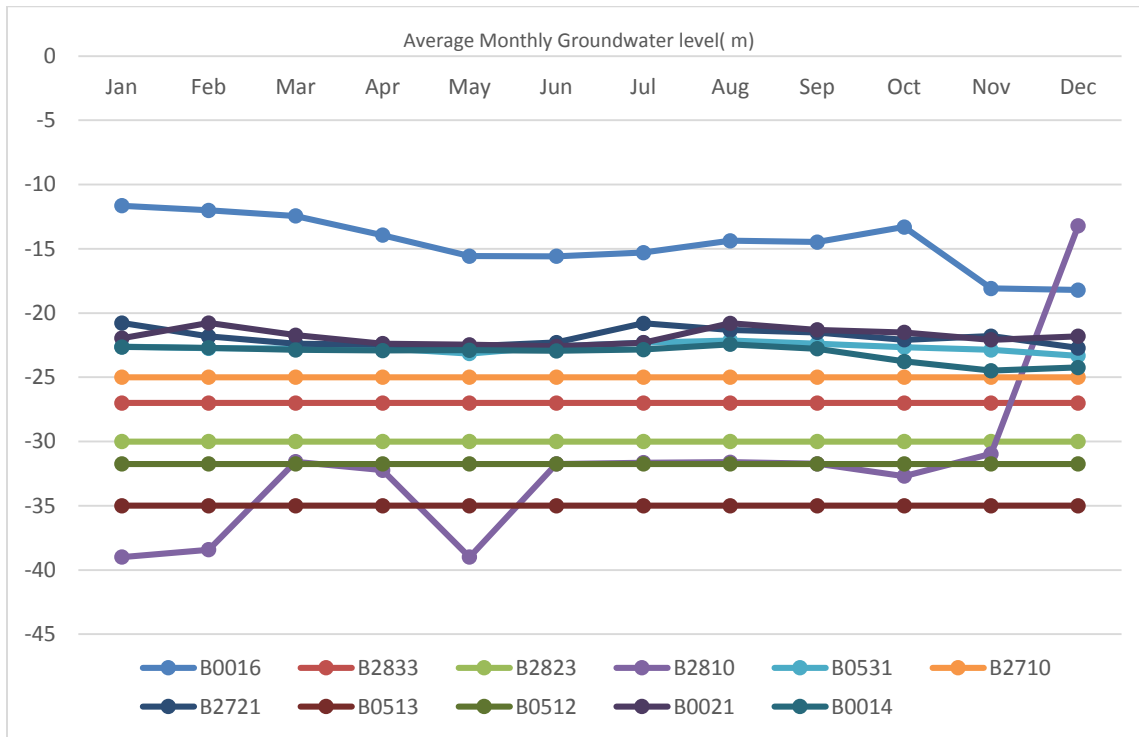


Figure 10 Average historical groundwater level below the earth surface(data from ERA over a period of 2012 to 2015)

### 3.2 Slope Stability Modelling

This part of the study focusses on limited landslide area where attempts were made to investigate the effect of groundwater level on the stability of a slope. The area is located on the boundary of the basalts. Highly weathered basalt is intercalated between the basalt and the limestone. It is sand or mud of soft particles prone to liquefying in the case of containing water. The layer is very soft and erosive, which would trigger slope collapses (GSE, 2016). The slope is under very high landslide zone (Shiferaw A, 2014).

The limestone that is fine to medium grained is widely distributed in the region. In addition to that, it reaches with Colluvial deposit, mainly composed of basalt boulders, gravel, sand, mud, and clay including black and organic soil as “black cotton soil”, which have come from the mountainous side cliff. Water permeability of the layer is relatively high. The deposit is a source of the rock falls and slope failures in the rainy season. (Geo-hazard Investigation Directorate, 2016)

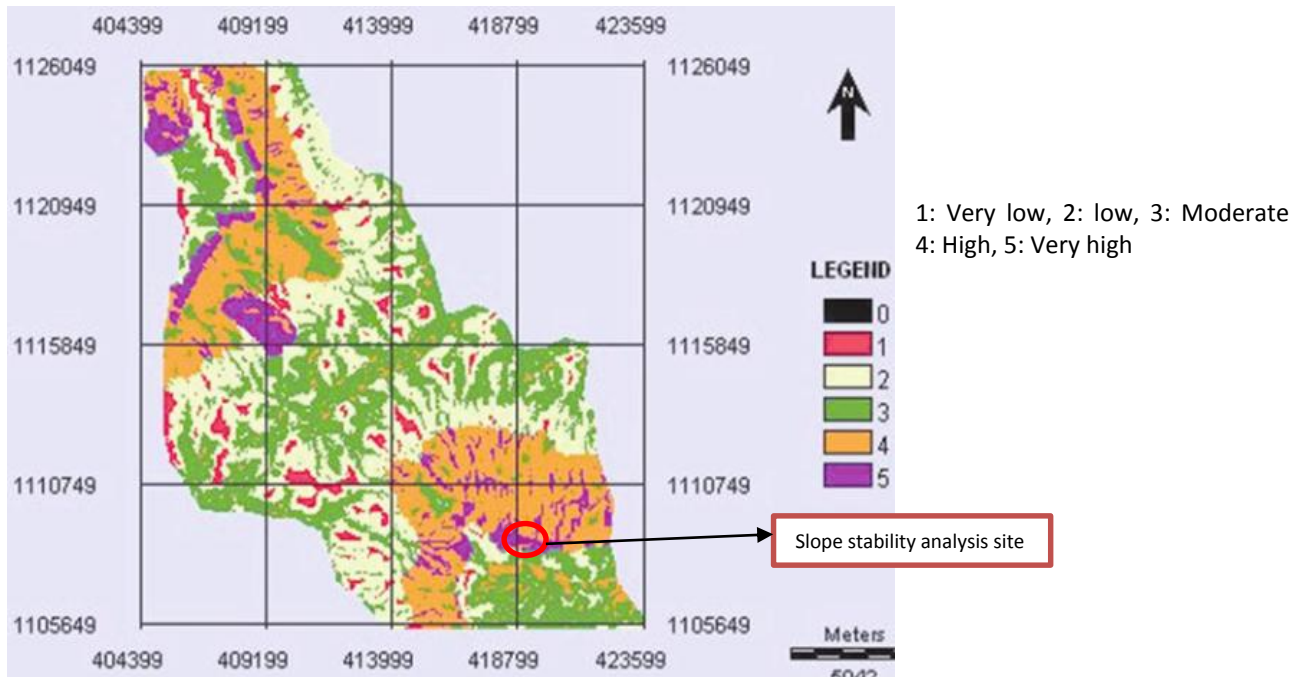


Figure 11 Landslide hazard zonation map of BNG (Shiferaw A, 2014)

The analysis was performed for a single slip surface as part of the failure back analysis using a module of GeoStudio 2012: SLOPE/W to calculate the factor of safety by Limit equilibrium method (LEM). LEM methods are the most widely used for analyzing slope stability. The simplicity and versatility of the LEM rest with the concept that the geometry of the potential failure surface in a slope is known and the slope can be discretized into finite vertical slices. Each slice is then analyzed using principles of force and/or moment equilibrium (Duncan, J.M., Wright, S.G., 2005) for its contribution to the stability of the slope.

## 4. Results and Discussion

### 4.1 Steady State Model Development and Simulation

The steady state flow is the state in which the volume passing a given point per unit of time remains constant. An initial steady state condition is required for time-dependent modelling of groundwater flow. The required data including recharge, initial hydraulic head, evapotranspiration, hydraulic conductivity etc. were imported into the model system. After feeding the data and running the model, the hydraulic heads are the primary results of MODFLOW in a steady state simulation as shown in Figure 14. Steady state simulation; the initial heads are used as starting values. Actual water table levels, obtained from the observation wells in the study area, were used to retrieve the initial water level. These same values were loaded into the model as initial hydraulic heads.

Eleven observation piezometers and selected springs, where the water level measurements were averaged to daily, were used for model simulation. The wells have different head value within a short distance difference between them. In addition to that, some wells show the comparatively significant difference in a year while others have approximately same groundwater level in all months of the year. Nevertheless, all measuring wells show a continuous increase in level from 2012 to 2014 except wells leveled as B2823 and B0513. Model simulations were completed over a daily period.

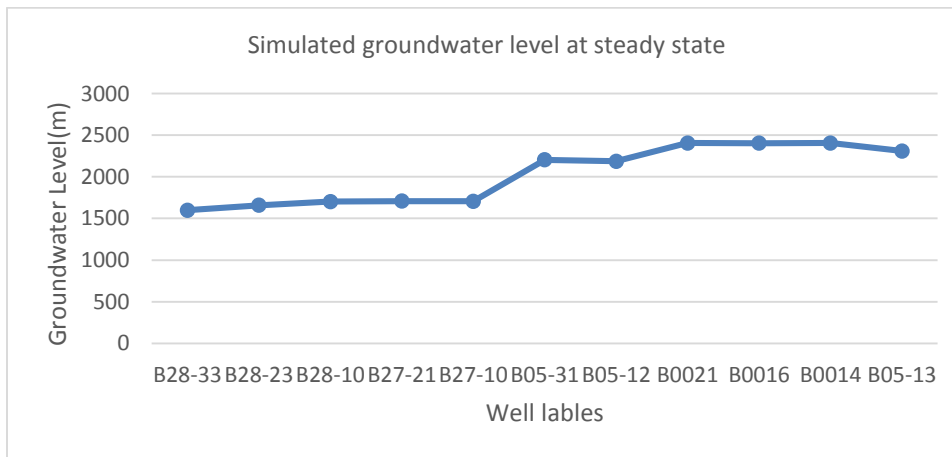


Figure 12 Simulated groundwater level at steady state

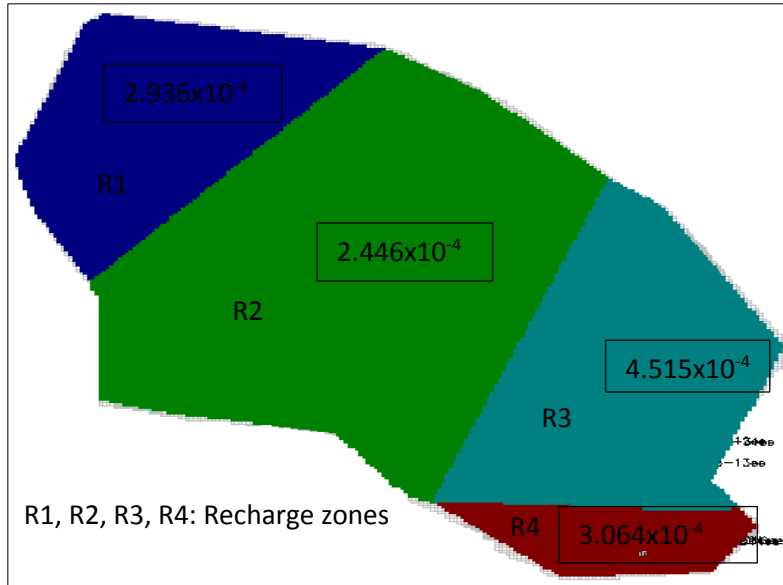


Figure 13 Recharge zones (not to scale) and values in m/day

#### 4.2 Transient Model Development and Simulation

Transient groundwater flow represents a dynamic system, in which variable inflows, outflows, and groundwater storage change with time. For transient calculations of groundwater flow, a stable initial condition, which is created from steady-state simulation, has been adopted. A specific yield of 0.0868 and specific storage of  $1.1 \times 10^{-3}$  were used. The time of one-year simulation, without sinks, is divided into twelve stress periods; each stress period represents a month, while the length of each stress period is divided into days. The total time steps, therefore, equal 12 months, while the total simulation time equals 365 days. Figure 14 shows the calculated head contours and flow directions.

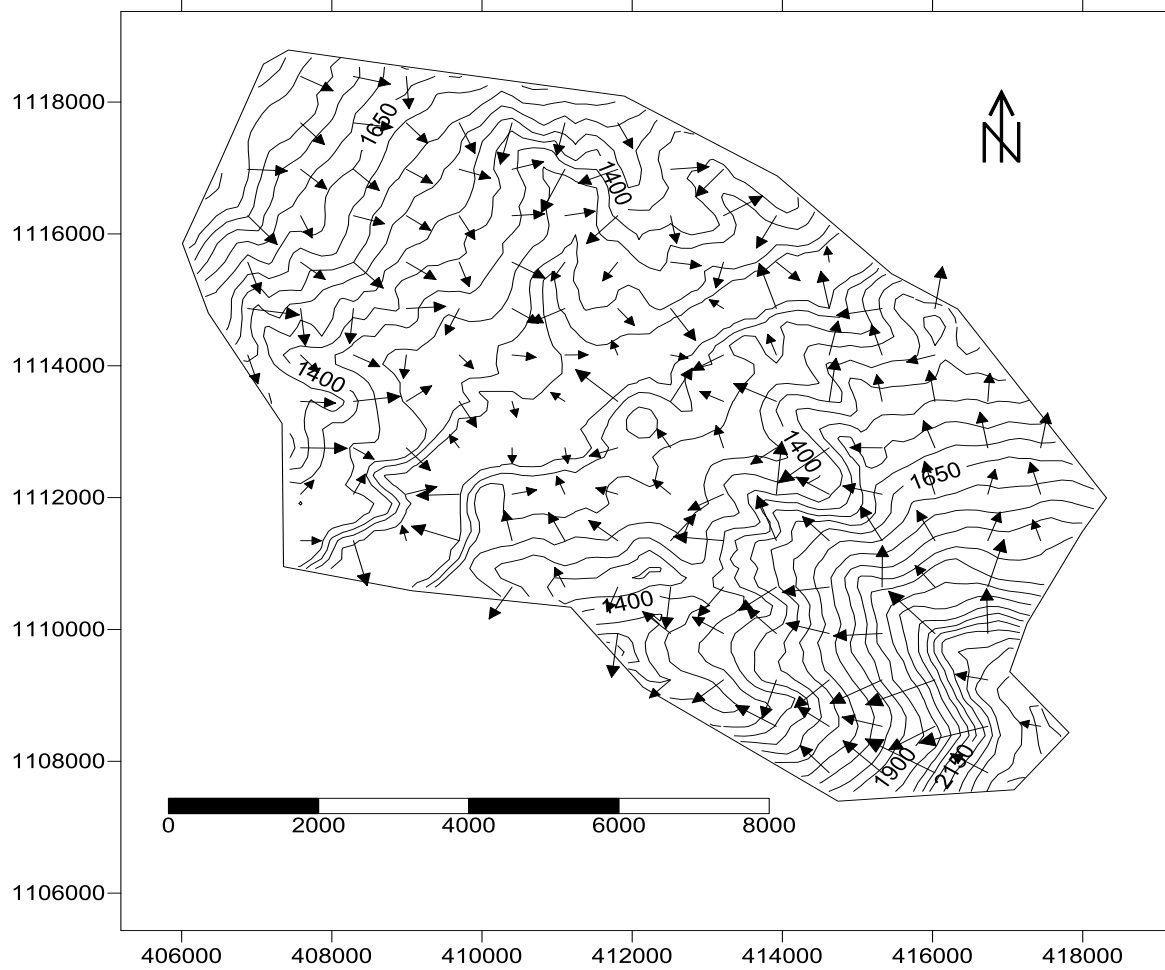


Figure 14 Contour of computed groundwater level at steady state

In addition to this, a model may be used to predict future estimates of the hydraulic response of an aquifer, under different scenarios, such as decrease/increase in recharge due to land use change. To predict by simulation, the aquifer condition after five years, the stress period of this duration should be divided into 60 stress periods: one-year simulation is divided into 12-period lengths. Variable groundwater levels were noticed at different locations of the aquifer but the variation of the level with time is very slow and minor. However, due to the bulkiness of the transient model result, we only showed selected stress period groundwater level result (Figure 15). Moreover, to test model results of one-year we remodelled it by dividing the year into only twelve stress periods and the results are included in figure 16.

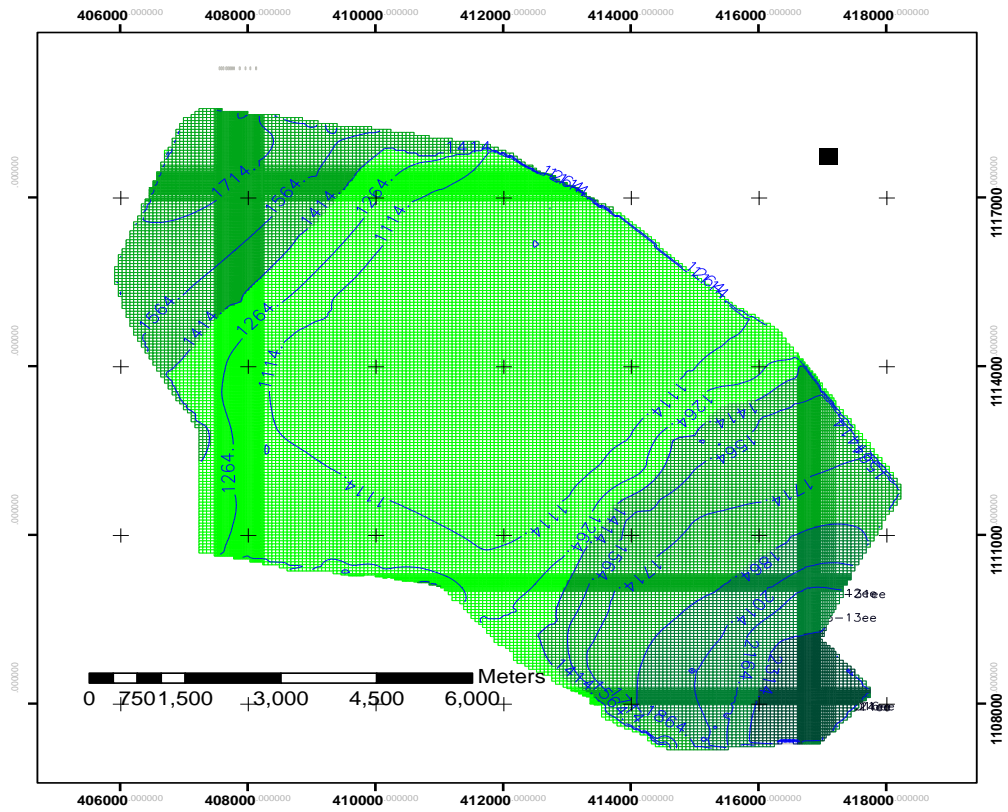


Figure 15 Contour of groundwater level at transient state for month of August (Stress period 8, time step 15)

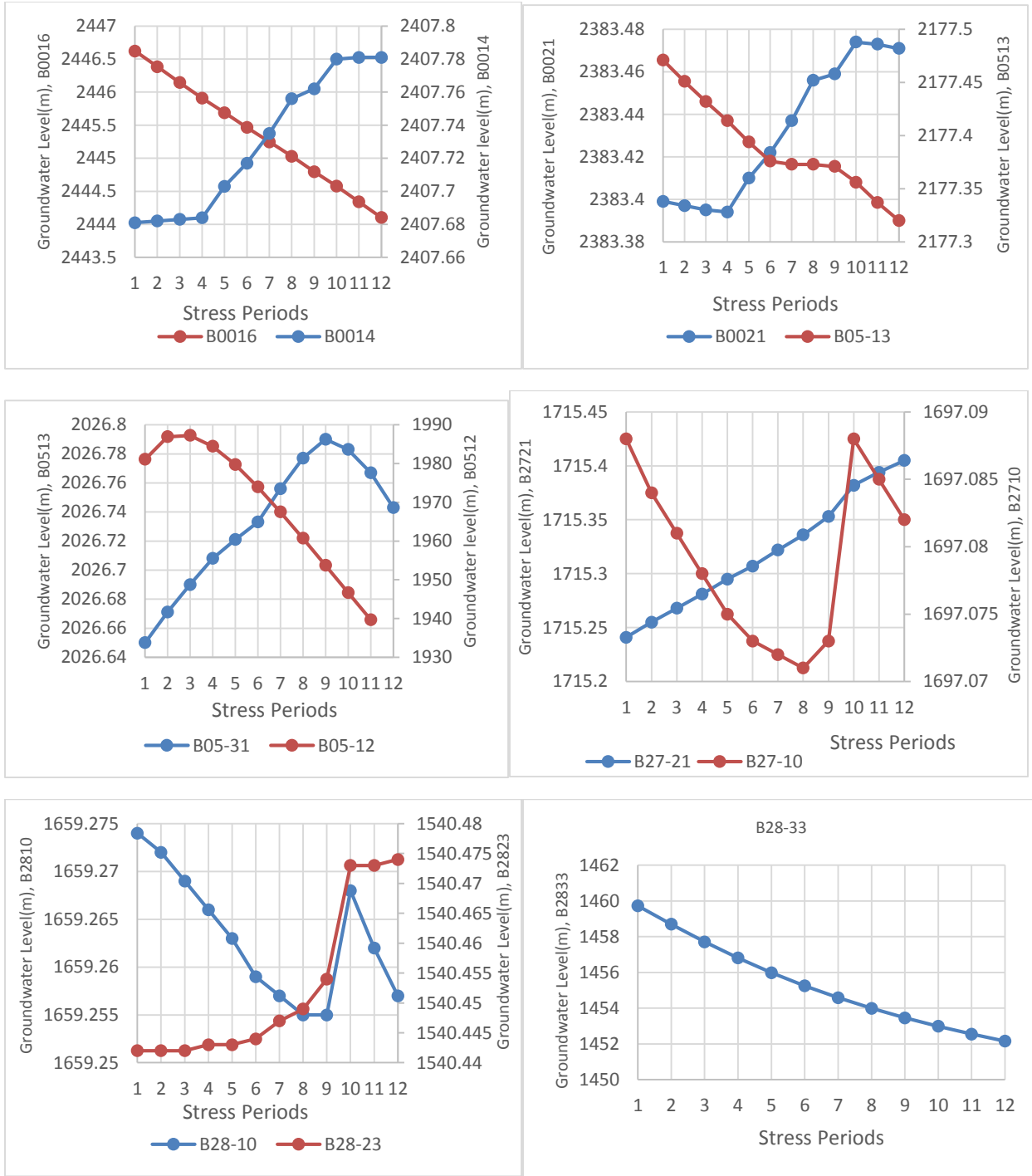


Figure 16 Simulated groundwater level at transient state

### 4.3 Slope Stability Analysis

After groundwater flow modelling calibration, we took the groundwater head for the specific selected slope to analyze the stability. Before we analysis the slope we plotted the historical landslide, groundwater, and rainfall of selected slope analysis site. The selected slope is conceptualized in a way that the result to be reasonable. The results of the analysis are presented and discussed in comparison with the historical landslide records.

Following the sensitivity analysis to assess the effects of mesh refinement, appropriate mesh configurations were determined for this site as shown in Figure 17. We used an unstructured triangular finite-element mesh. This mesh was developed so that nearly all elements would be equilateral or isosceles right triangles, which are highly desirable to improve computational accuracy.

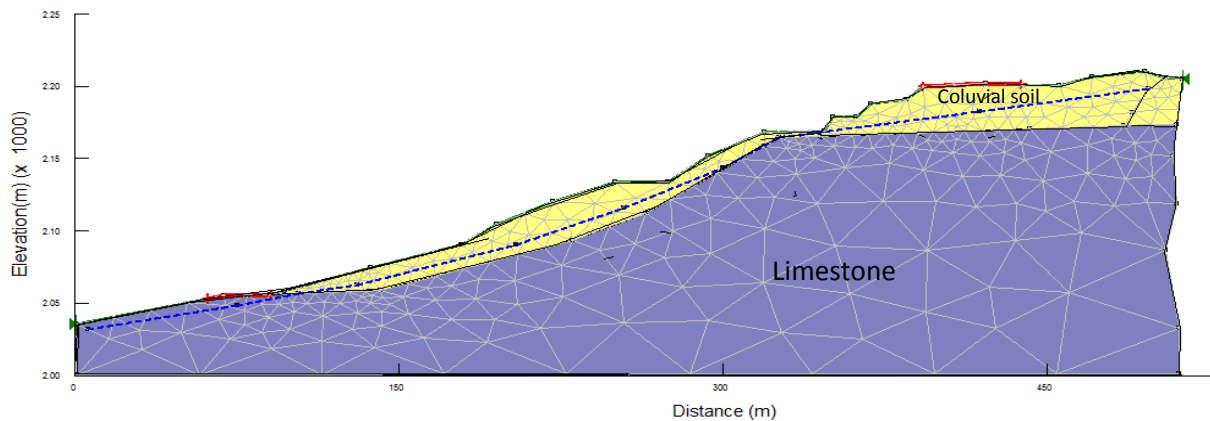


Figure 17 Gridded Slope geometry, material used and position of pore-water pressure line in the specific slope

The important parameters in the hydro-mechanical framework are the drained cohesion  $c'$  and friction angle  $\phi'$  defined in the Mohr-Coulomb failure criterion. Direct shear tests were conducted under saturated conditions in order to obtain shear strength parameters of soil. The values for these hydro-mechanical properties are listed in the following table.

Table 3 Hydro-Mechanical Parameters

Material I		Material II	
lab result	Adjusted for the model	lab result	Adjusted for the model
$\gamma = 20.50\text{KN/M}^3$	21	$\gamma = 20.00\text{KN/M}^3$	20.6
$\phi_{ef} = 26.5.00$	28.8	$\phi_{ef} = 26.5.00$	26.6
$C_{ef} = 6.00\text{ Kpa}$	10	$C_{ef} = 0.00\text{ Kpa}$	6

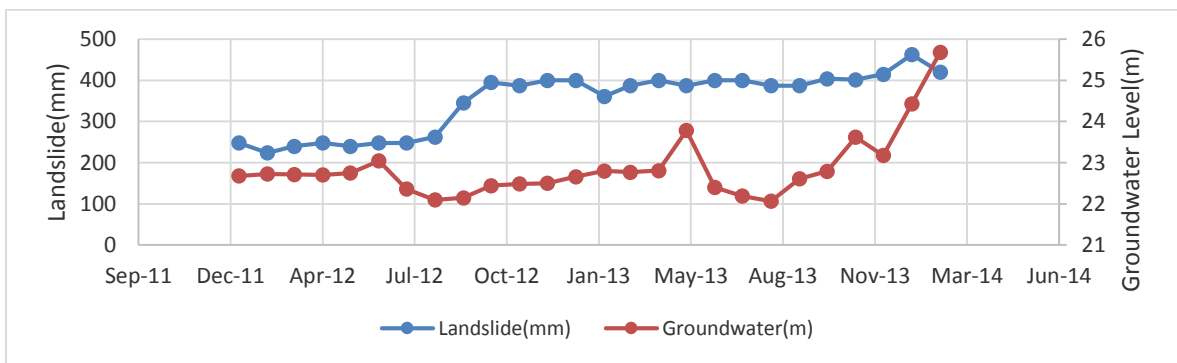
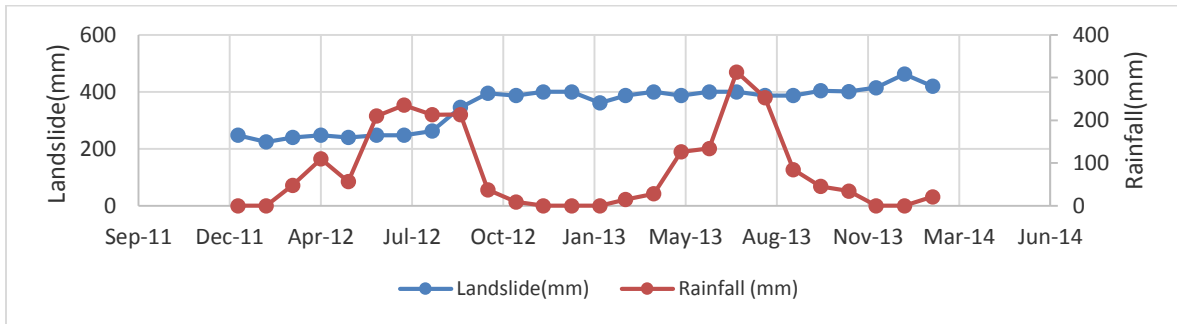
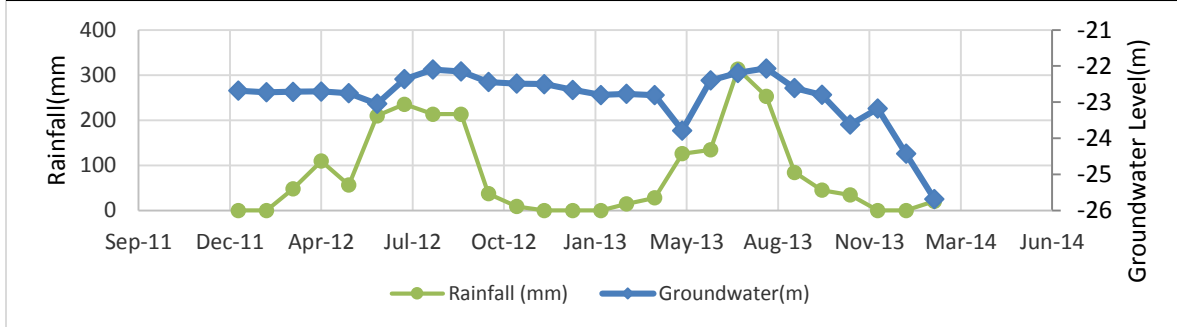


Figure 18 Time trend of rainfall groundwater level and landslide at selected very high landslide zone of the region (Filiklik rainfall station and Pizo-metre B05-13)

The key indicator in slope stability analysis is the factor of safety (FS), which is commonly defined as the ratio of the resisting shear force to the driving shear force along a failure surface. FS is equal to one means resistance forces and sliding forces are balanced. If FS is, greater than one means the landslide is stable while FS less than one is unstable or sliding. A method of slices was used to compute the FS along failure surfaces and to search a critical slip surface (a surface with the lowest FS).

$$FS = \frac{\text{Resistance force against landslide soil mass}}{\text{Force when landslide soil mass starts sliding along the slip surface}}$$

We have analyzed the historical groundwater level-rainfall, groundwater level-landslide and rainfall-landslide records at the specific site (as shown in Figure 18) in order to able to understand and evaluate the slopes stability model results. Moreover, initially, we examined the effects of topography and geology by using heterogeneous material properties, as defined by stratigraphy, without pore pressures. In this scenario, the least stable area is located on the steeper slope. The minimum FS obtained from the analysis is 1.228

For the second analysis pore-water, pressure field is taken from the result of MODFLOW and incorporated into the model. We obtain a realistic model of land sliding by combining pore pressures with heterogeneous strength properties. The result shows the least stable area where pore pressure is locally elevated in and the slope is relatively steeper. Figure 20 shows strength and water pressure plummet and upswing considerably at the different longitudinal profile of the slope geometry. We analyzed the effect of pore-water development and after many trials; it is noticed that it has the capability to reduce the FS up to 18 to 22 percent. In addition, every half a metre increase in groundwater level reduces the FS by 0.84 percent. We compared our results with records of past landslides. The plots show no clear relationship in rainfall, groundwater and landslide at this selected landslide site. Specifically, if we examine Figure 18 it is difficult to tell the relationship. However, if we take a closer look at the trend we can see that the difference in the level of these parameters is time. They have a strong relationship, especially the groundwater level rise and landslide measurements.

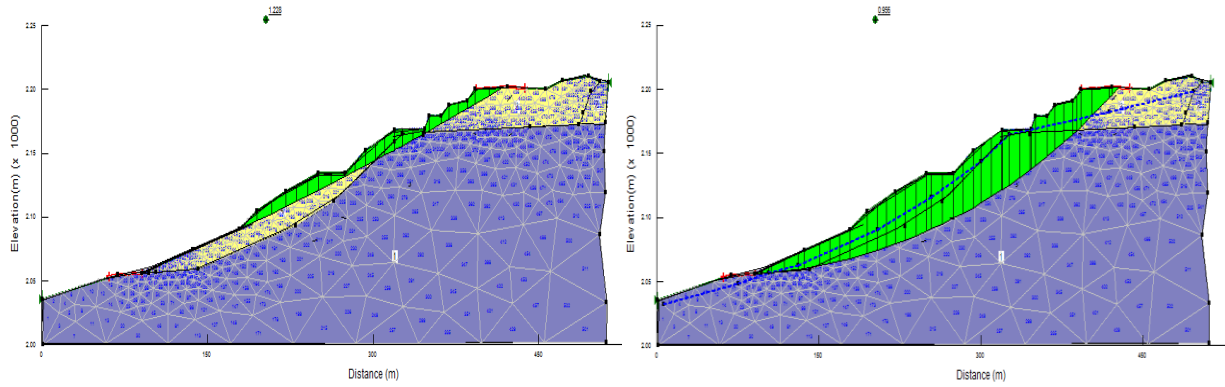


Figure 19 Slope stability analysis results (on the left slope analysis with no pore-water pressure and on the right with pore-water pressure imported from MODFLOW at steady state)

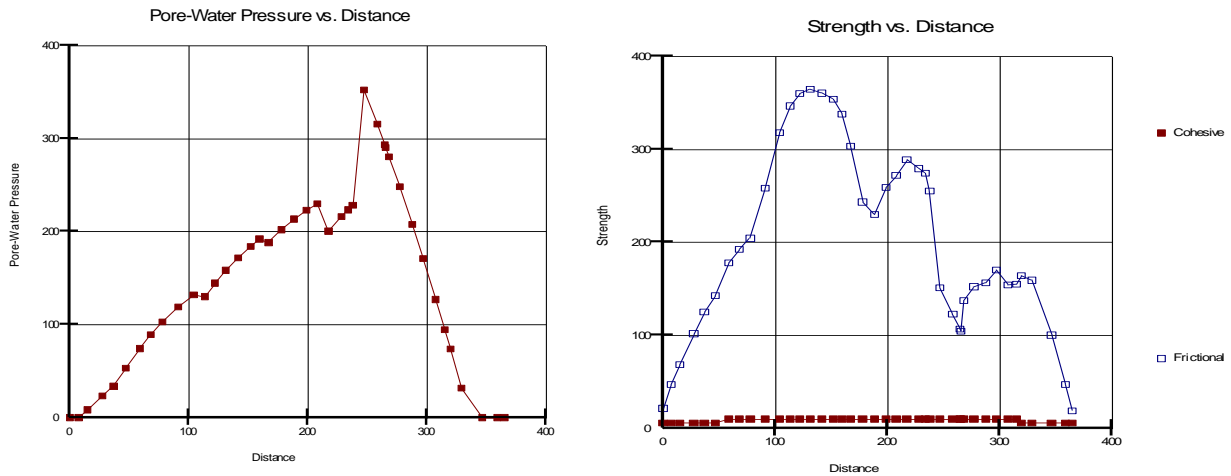


Figure 20 Pore-water Pressure and strength along the slope

Since the groundwater level variation from time to time is not uniform in the area, we could not capture the slope stability (FS) variation in the conceptualized model resolution. However, we tested (ten trials) the slope for an approximately equal change of groundwater level (less than 0.021 percent increase) and we observed the following changes in FS.

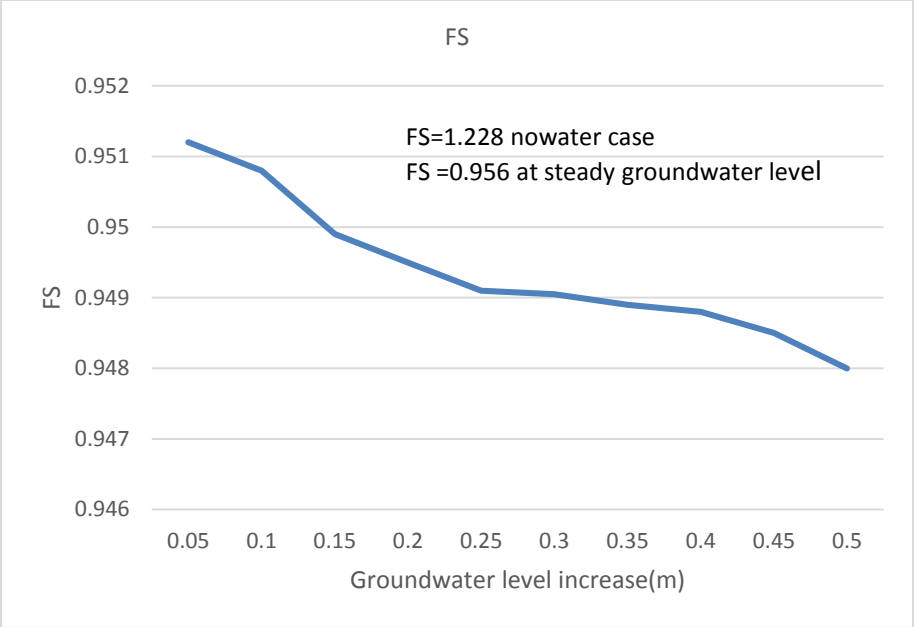


Figure 21 Impact of groundwater level rise on FS of the slope

## 5. Model Calibration

Model calibration is generally defined as the process of tuning a model for a particular problem or case by manipulating the input parameter, and initial or boundary conditions, within reasonable ranges until the simulated model results closely match the observed variables. The general approach in model calibration is to select some merit or objective function that is a measure of the agreement between measured and modelled data, and that is indirectly or directly related to the adjustable parameters. The best-fit parameters are obtained by minimizing the objective function. Model calibration, i.e., minimization of the merit function, can be achieved by trial and error or, as is becoming more popular, by using an automated minimization or parameter estimation technique. A model is considered calibrated when it reproduces data within some subjectively acceptable level of precision.

In this study, there was no local information about the values of hydraulic conductivity. It should be estimated based on the observed head and other hydrogeological parameters. Therefore, the area is zoned into twelve main lateral geological formations of the aquifer and the hydraulic conductivity values on these zones were defined as unknown parameters. On all zones,  $1 \times 10^{-7}$ , 100, and 0.01m/day were specified as the minimum, maximum, and initial values respectively in order to get optimized parameters using parameter estimation (PEST) model.

PEST is an inverse model used to determine the value of a parameter such as hydraulic conductivity or recharge by using observation data, for example, piezo-metric head or stream flow. Regularized inversion problems are most commonly addressed by use of the parameter estimation code PEST (Doherty, 2010a). PEST is an open-source, public-domain software suite that allows model-independent parameter. The inverse model tries to estimate the optimum value of the parameters by minimizing the residual. The objective functions are calculated as the sum of squared weighted residuals or as mean square error (MSE) (John E. Doherty, and Randall J. Hunt, 2010).

$$MSE = \frac{1}{n} \sum_{i=1}^n (H_c - H_o)^2$$

Where; n = number of data;  $H_c$  = computed value; and  $H_o$  = observed value.

At each iteration, parameter sensitivities were also computed by the PEST model. This allows the user to distinguish sensitive and insensitive parameters, and consequently, depending on the approach used, the size of zones can be modified in order to use the computation time more effectively. Several modifications in the size of zones were made throughout the simulations in order to balance the sensitivities. In the end, a reasonable fit was obtained between observed and computed piezo-metric heads. In Figure 22 Measured head versus observed head is shown after calibration. The coefficient of determination ( $R^2$ ) was calculated as =0.9984 at steady state simulation and a minimum of 0.9781 at transient simulation. Some of the plots of calculated head versus observed head at transient state are shown in Figure 24 and the rest are in the appendix section of the paper. There is generally a good agreement between observed and computed values. Overestimates and underestimates are evenly distributed.

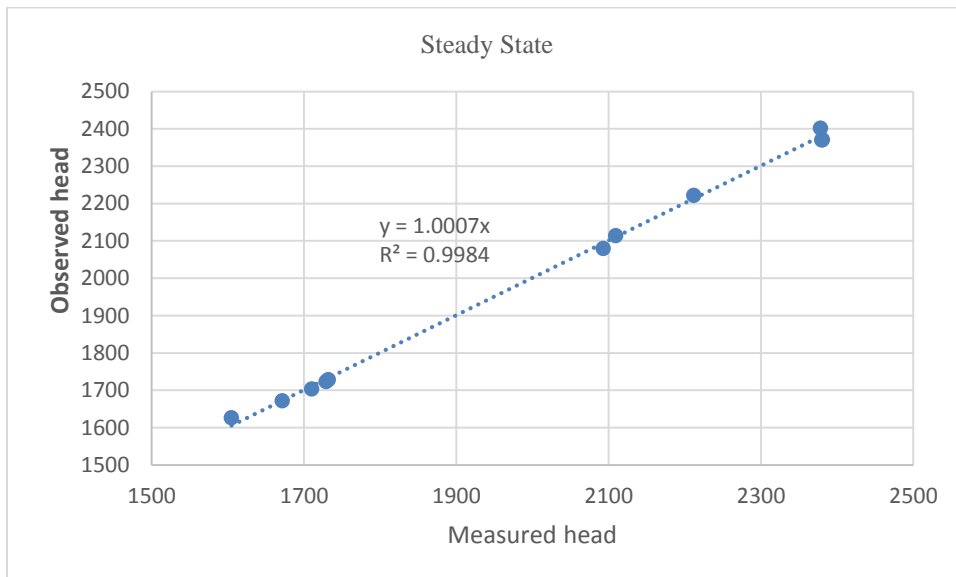


Figure 22 Measured head versus observed head at steady state

The model was calibrated in a two-step process, first using steady-state simulations to estimate hydraulic conductivities of the model layer to match measured heads and flows at target wells, then using a transient simulation to estimate the parameters that predominantly affect fluctuations in flow. The model used a hydraulic conductivity within a range of 0.002 m/day to 19.82 m/day.

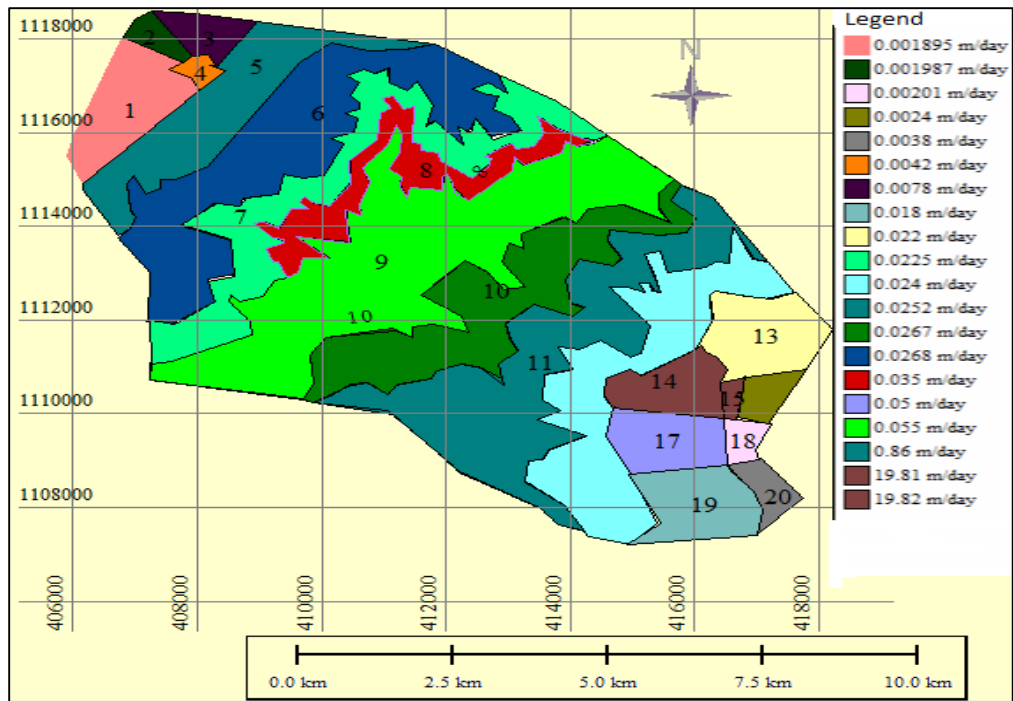


Figure 23 Hydraulic conductivity of the area after calibration

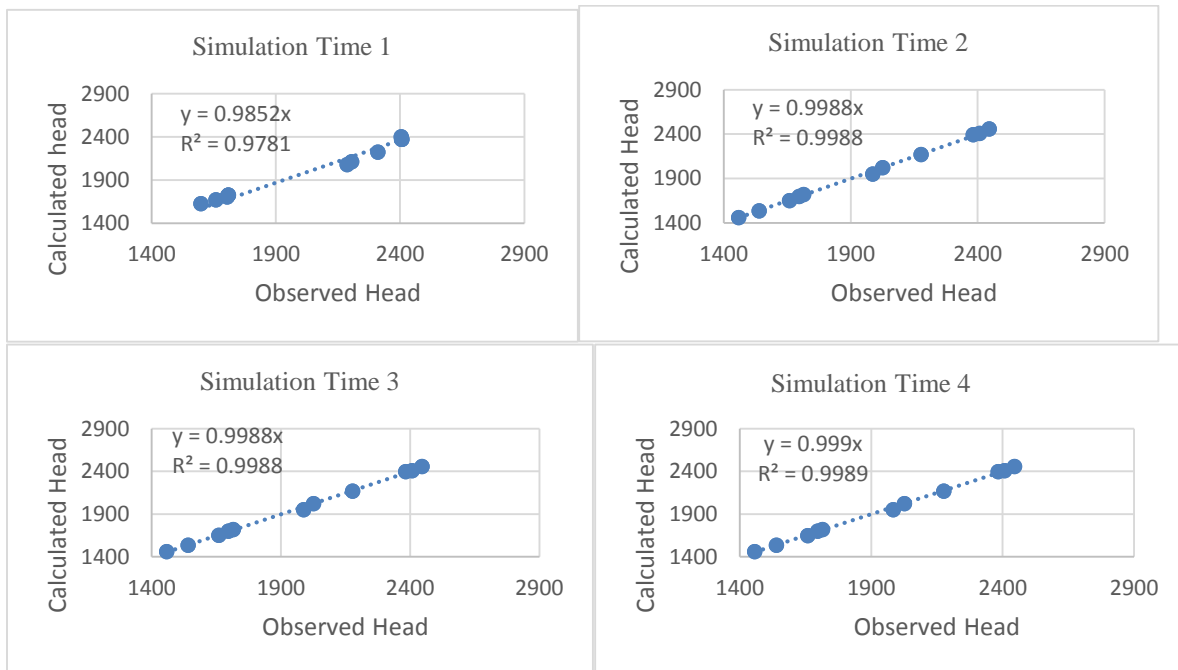


Figure 24 Measured head versus observed head at transient state

Calibrated values from the steady state analysis were then used in attempts to calibrate the model using transient conditions, which included adjusting stream conductance, recharge, evapotranspiration, and storage coefficients. Calibration of the transient simulation yielded estimates of storage coefficients in the upper layers and estimates for stream conductance. The time of one-year simulation, without sinks, is divided into twelve stress periods; each stress period represents a month, while the length of each stress period is divided into days. The total time steps, therefore, equal 12 months, while the total simulation time equals 365 days. There were some verification data of two months. The available data were used to calibrate the transient state of the model. The first step of the calibration was to assign an initial value for storage coefficients and specific yield for the model layer. Calibration is done using trial and error procedure by changing the specific yield, storage coefficient, and with a very limited range of the hydraulic conductivity values. Good performance of the model was observed through the transient simulation to fit between simulated and observed head in the observation wells.

The calibrated result of the model also checked on the water budget the region at both steady state and transient state.

Table 4 Water budget of the model at steady state flow simulation

Time Step 1 of Stress Period 1, Water Budget of the Whole Model Domain :			
Flow Term	In	Out	In-Out
Storage	0.000e+00	0.000e+00	0.000e+00
Constant Head	1.188e+04	3.596e+04	-2.408e+04
Wells	6.546e+03	0.000e+00	6.546e+03
Drains	0.000e+00	6.661e+02	-6.661e+02
Recharge	1.853e+04	0.000e+00	1.853e+04
ET	0.000e+00	8.858e-01	-8.858e-01
River Leakage	9.009e-04	3.239e+02	-3.239e+02
Head Dep Bounds	0.000e+00	0.000e+00	0.000e+00
Stream Leakage	0.000e+00	0.000e+00	0.000e+00
Interbed Storage	0.000e+00	0.000e+00	0.000e+00
Reserv.L Leakage	0.000e+00	0.000e+00	0.000e+00
<b>Sum</b>	<b>3.695e+04</b>	<b>3.695e+04</b>	<b>-8.237e-01</b>
<b>Discrepancy [%]</b>	<b>0</b>		

Table 5 Water budget of the model at transient state of flow

<b>Time Step 1 of Stress Period 1, Water Budget of the Whole Model Domain :</b>			
<b>Flow Term</b>	<b>In</b>	<b>Out</b>	<b>In-Out</b>
Storage	1.2483e+07	1.2500e+07	-1.6699e+04
Constant Head	1.3680e+04	2.3001e+04	-9.3211e+03
Wells	7.0310e+03	0.0000e+00	7.0310e+03
Drains	0.0000e+00	0.0000e+00	0.0000e+00
Recharge	1.8650e+04	0.0000e+00	1.8650e+04
ET	0.0000e+00	3.7281e-04	-3.7281e-04
River Leakage	1.9798e-02	1.2733e+02	-1.2731e+02
HeadDep.Bounds	0.0000e+00	0.0000e+00	0.0000e+00
Stream Leakage	0.0000e+00	0.0000e+00	0.0000e+00
Interbed Storage	0.0000e+00	0.0000e+00	0.0000e+00
Reserv.L Leakage	0.0000e+00	0.0000e+00	0.0000e+00
<b>Sum</b>	<b>1.2522e+07</b>	<b>1.2523e+07</b>	<b>-4.6630e+02</b>
<b>Discrepancy</b>	<b>0</b>		
<b>[%]</b>			

## 6. Conclusion and Recommendation

The role of groundwater flow model is to characterize the balance of withdrawal or recharge events so that changes in local groundwater flow rates and changes in water levels can be predicted. Regardless, in mountainous regions of Ethiopia, the scholar work on groundwater is relatively low due to several reasons such as inadequate data, the complexity of aquifer geometry and inaccessibility of the area. In this paper groundwater table fluctuation in unconfined aquifer principally due to rainfall infiltration, recharge from the surrounding, interaction with the river was modelled.

Modelling is an extensively used method of studying and quantifying such responses of an aquifer. Performed steady and transient states modelling of groundwater flow were based on parameters after calibration. The calibration results using PEST are good at steady state groundwater flow modelling, but in the transient state, it was challenging even to finish the simulation, it terminates abnormally. The reason behind this difficulty primarily raised from persistent instability problems apparently caused by large variations in groundwater-surface water interaction between iterations of the solver. This resulted in long execution times and elevated residual estimates. The transient model proved inherently unstable. Due to temporal transitions from groundwater discharging to surface water recharging the aquifer, the model would not converge longer time step, and could only be calibrated using a solution algorithm (PCG2) that would allow for non-convergence at any particular time step and proceed to the next.

Following that, we obtained a reasonable variation of groundwater table in response to the above-mentioned stresses. The results show that groundwater table is varying depending mainly on recharge from the hilly side of the extent. There is a contribution from rainfall infiltration too but it is trivial especially on Dejen side of the gorge. However, in a limited section of the region, the upsurge and drop of groundwater level during rainfall and dry seasons are noteworthy. The amount of level difference in the area between the driest and wettest time is not significant except at limited regions.

In addition to that, this work exhibited; though, in limited areas the recharge is high into the aquifer and may contribute to the slope instability at slopes that are classified as high landslide hazard zones, in the majority of the regional groundwater stays stable throughout the year. Which implies

that the rainfall infiltration in these sites has less effect on stability. Their geographical location, sensitivity analysis, and geological zone imply that they are receiving water from northeast and southwest neighbor of the proposed model.

Model results and field measurements show the geometry is in continuous movement. A slight rise in water level decreases the FS of the slope substantially. Less than half a meter increase in water level, decrease the FS by nearly 0.84 percent. Moreover, it is understandable that the pore-water development corresponds to the slope of the area.

From this study, we can conclude that in order to make the investigation of slope instability and mitigation measures coupling groundwater flow modelling and slope stability models together with other triggering factors is economical and efficient. However, this process is not effective unless reliable data is collected and the area is conceptualized prudently. It is also apparent that this specific site needs further investigation of hydrogeology on both sides of the BNG independently since this study showed that the recharge and groundwater level fluctuation on the north and south of the river are dissimilar.

## 7. References

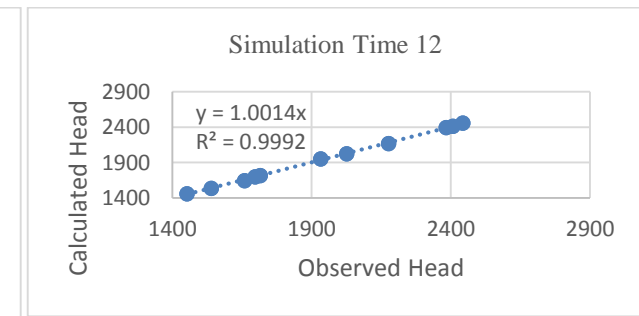
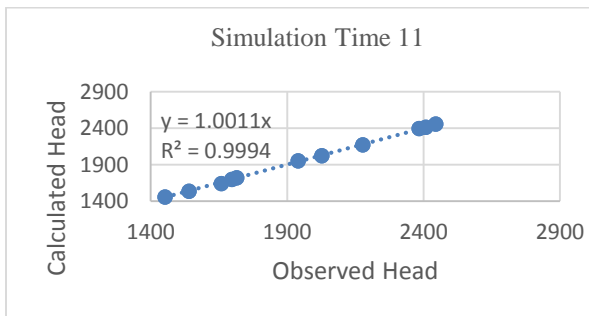
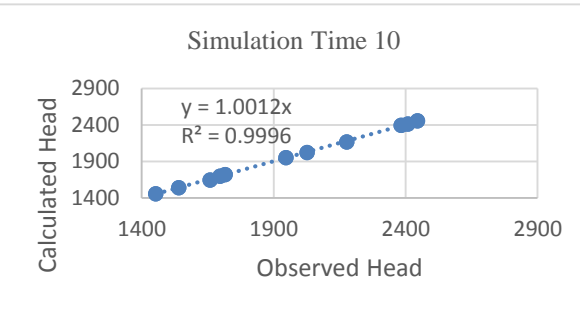
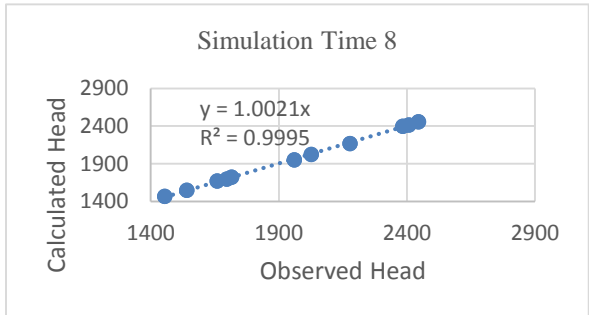
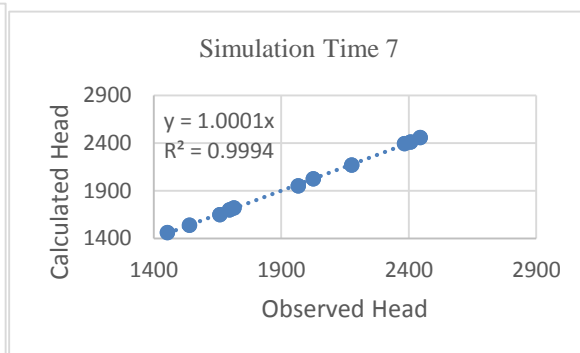
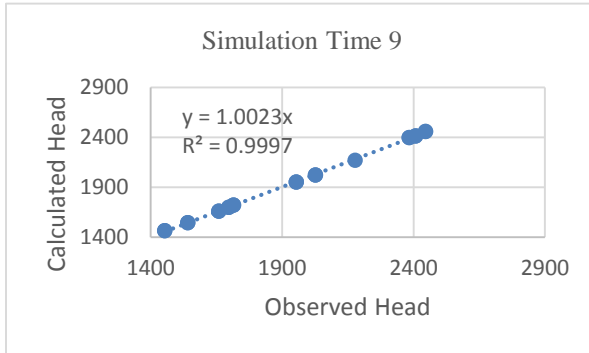
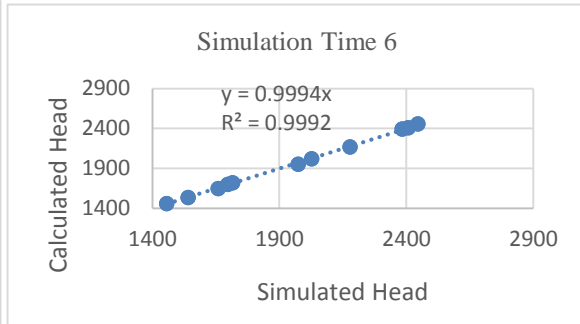
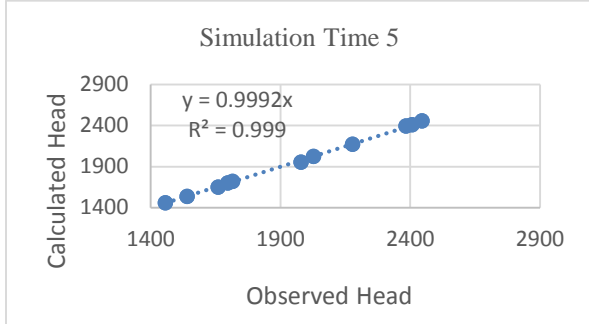
- Meten M et al. (2015). Effect of Landslide Factor Combinations on the Prediction Accuracy of Landslide Susceptibility Maps in the Blue Nile Gorge of Central Ethiopia. *Geoenvironmental Disasters*, 2(1), 9.
- Mondal, M.S. and Wasimi, S.A. (2006). Generating and forecasting monthly flows of the Ganges river with PAR model. *Journal of Hydrology*, 323(1-4), 41-56.
- Surinaidu L. et al. (2015). Application of MODFLOW for groundwater Seepage Problems in the Subsurface Tunnels. *J. Ind. Geophys.*, 422-443.
- Asmerom, G. H. (2008). Groundwater contribution and recharge estimation in the Upper Blue Nile flows, Ethiopia. *ITC MSc thesis, The Netherlands*.
- ASTM. (2010). Standard Guide for Application of a Ground-Water Flow Model to a Site-Specific Problem. *D5447-04*.
- Ayalew L and Yamagishi H. (2003). Slope failures in the Blue Nile basin, as seen from landscape. *Geomorphology*, 1361:1–22.
- Ayalew, L. (2000). Factors affecting slope stability in the Blue Nile basin. In *Landslides in Research, Theory and Practice: Proceedings of the 8th International Symposium on Landslides held in Cardiff on 26–30 June 2000 (pp. 1-101)*. Thomas Telford Publishing.
- Ayalew, L. M. (2009). Geotechnical aspects and stability of road cuts in the Blue Nile Basin, Ethiopia. *Geotechnical and Geological Engineering*, 27(6), 713-728.
- Calvello, M. C. (2008). A numerical procedure for predicting rainfall-induced movements of active landslides along pre-existing slip surfaces. *International journal for numerical and analytical methods in geomechanics*, 32(4), 327-351.
- Chiang, W. H., and Kinzelbach, W. (1998). Processing Modflow: A simulation program for modelling groundwater flow and pollution. In *User manual*.
- Corsini, A. F. (2006). Space-borne and ground-based SAR interferometry as tools for landslide hazard management in civil protection. *International Journal of Remote Sensing*, 27(12), 2351-2369.
- Debieche, T. H. (2002). Hydrological and hydrochemical processes observed during a large-scale infiltration experiment at the Super-Sauze mudslide (France). *Hydrological Processes*, 26(14), 2157-2170.
- Doherty, J. (2010a). *PEST, Model-independent parameter estimation—User manual (5th ed., with slight additions)*. Brisbane, Australia: Watermark Numerical Computing.
- Duncan, J.M., Wright, S.G. (2005). *Soil Strength and Slope Stability*. John Wiley & Sons Inc.
- Gasmo, J. M. (2000). Infiltration effects on stability of a residual soil slope. *Computers and Geotechnics*, 26(2), 145-165.

- Geo-hazard Investigation Directorate, G. S. (2016). *Slope Instability Investigation and Core Drilling Work” at Gohatsion - Dejen Road Segment, Amhara and Oromia National Regional State*. Addis Ababa: Geological Survey of Ethiopia.
- GSE. (2016). *Slope stability investigation*. Addis Ababa.
- Guglielmi, Y. V. (2002). Hydrogeochemistry: an investigation tool to evaluate infiltration into large moving rock masses (case study of La Clapière and Séchilienne alpine landslides). *Bulletin of Engineering Geology and the Environment*, 61(4), 311-324.
- H, A. L. (2004). Slope failures in the Blue Nile basin, as seen from landscape evolution perspective . *Geomorphology* 57 , 95-116.
- Harbaugh, A. W. (2005). *MODFLOW-2005, the US Geological Survey modular ground-water model: the ground-water flow process (pp. 6-A16)*. Reston, VA, USA: US Department of the Interior, US Geological Survey.
- Harbaugh, A. W., Banta, E. R., Hill, M. C., and McDonald, M. G., (2000). the US Geological Survey modular ground-water model: User guide to modularization concepts and the ground-water flow process . In *MODFLOW2000*. US Geological Survey Reston.
- Henok Woldegiorgis, T. K. (2014). LANDSLIDE HAZARD ZONATION USING EXPERT EVALUATION TECHNIQUE: A CASE STUDY OF THE AREA BETWEEN GOHATSION TOWN AND THE ABAY (BLUE NILE) RIVER, CENTRAL ETHIOPIA. *SINET: Ethiop. J. Sci.*, 37(2):75–94.
- Hong, Y. M. (2011). Forecasting groundwater level fluctuations for rainfall-induced landslides. *Natural Hazard*, 57(2), 167-184.
- Iverson, R. M. (2000). Landslide triggering by rain infiltration. *Water resources research*, 36(7), 1897-1910.
- Jiao, J. J. (2005). Confined groundwater zone and slope instability in weathered igneous rocks in Hong Kong. . *Engineering Geology*, 80(1), 71-92.
- John E. Doherty, and Randall J. Hunt . (2010). *Approaches to Highly Parameterized Inversion: A Guide to Using PEST for Groundwater-Model Calibration* . Reston, Virginia: U.S. Department of the Interior, U.S. Geological Survey.
- Johnson, K. A. (1990). Hydrologic conditions leading to debris-flow initiation. *Canadian Geotechnical Journal*,, 27(6), 789-801.
- Kebede, S. (2012). *Groundwater in Ethiopia: Features, numbers and opportunities*. Springer Science & Business Media.
- Kjekstad, O. &. (2009). Economic and Social Impacts of Landslides. In C. P. Sassa K., *Disaster Risk Reduction*. Springer, Berlin, Heidelberg.
- Konikow, L. F., and Mercer, J. W. ( 1988). Groundwater Flow and Transport Modeling. *Journal of Hydrology*, v. 100, p. 379-409.

- Leroueil, S. &. (1996). Importance of strain rate and temperature effects in geotechnical engineering. In Measuring and modeling time dependent soil behavior . *ASCE*, 1-60.
- Matebie Meten, N. P. (2014). The Application of Weights of Evidence Modelling for Landslide Susceptibility Mapping of Dejen-GohaTsiyon Transect in the Blue Nile Gorge, Central Ethiopia. *International Symposium Geohazards: Science, Engineering and Management, Kathmandu, Nepal*, Paper No. LF-04.
- McDonald, M. G. (1988). *McDonald, M. G., & Harbaugh, A. W. (1988). A modular three-dimensional finite-difference ground-water flow model.*
- Mercer, J. W., and Faust, C. R. ( 1980). Ground -Water Modeling: An Overviewa:. *Ground Water*, v. 18, no. 2 , p. 108-115.
- Ng, C. W. (1988). A numerical investigation of the stability of unsaturated soil slopes subjected to transient seepage. *Computers and geotechnics*, 22(1), 1-28.
- Rahardjo, H. L. (2001). The effect of antecedent rainfall on slope stability. In Unsaturated Soil Concepts and Their Application in Geotechnical Practice. *Springer Netherlands*, 371-399.
- Richards. (1931.). Capillary conduction of liquids through porous mediums. *J. Appl.physi*, 1 (5), 318–333.
- Saed, J. (2005). Slope stability studies along Gohatsion Dejen Road. *MSc Thesis, Addis Ababa University*.
- Shiferaw A, T. K. (2014). Landslide hazard zonation map of Abay Gorge. *Landscape Ecology and Water Management: Proceedings of IGU Rohtak* (pp. 15-32). illus: Springer.
- Sidle, R. C. (2006). Landslides: processes, prediction, and land use. *American Geophysical Union, Vol 18*.
- Tsagaras, I. R. (2002). Controlling parameters for rainfall-induced landslides . *Computers and geotechnics*, 29(1), 1-27.
- Van Asch, T. W. (1999). A view on some hydrological triggering systems in landslides. . *Geomorphology*, 30(1), 25-32.
- van Asch, T. W. (2007). Techniques, issues and advances in numerical modelling of landslide hazard. *Bulletin de la Société géologique de France*. 178(2), 65-88.
- Woldearegay, K. (2013). Review of the occurrences and influencing factors of landslides in the highlands. *Momona Ethiopian Journal of Science (MEJS)* , V5(1):3-31 .
- Woldegiorgis H. (2008). Landslide hazard zonation mapping in Blue Nile Gorge. *MSc. Thesis, Addis Ababa University, Addis Ababa*.

# Appendix

## Appendix A: Calculated head vs observed head plots



Appendix B: Water budget of the model at different simulation times

TIME STEP 1 OF STRESS PERIOD 1				
=====				
WATER BUDGET OF THE WHOLE MODEL DOMAIN:				
=====				
FLOW TERM	IN	OUT	IN-OUT	
STORAGE	1.2561328E+07	1.2578414E+07	-1.7086000E+04	
CONSTANT HEAD	1.3680353E+04	2.3005346E+04	-9.3249932E+03	
WELLS	7.0310000E+03	0.0000000E+00	7.0310000E+03	
DRAINS	0.0000000E+00	0.0000000E+00	0.0000000E+00	
RECHARGE	1.8642516E+04	0.0000000E+00	1.8642516E+04	
ET	0.0000000E+00	3.7280540E-04	-3.7280540E-04	
RIVER LEAKAGE	1.9798229E-02	1.2732978E+02	-1.2730998E+02	
HEAD DEP BOUNDS	0.0000000E+00	0.0000000E+00	0.0000000E+00	
STREAM LEAKAGE	0.0000000E+00	0.0000000E+00	0.0000000E+00	
INTERBED STORAGE	0.0000000E+00	0.0000000E+00	0.0000000E+00	
RESERV. LEAKAGE	0.0000000E+00	0.0000000E+00	0.0000000E+00	
SUM	1.2600682E+07	1.2601547E+07	-8.6478790E+02	
DISCREPANCY [%]	-0.01			

TIME STEP 1 OF STRESS PERIOD 2				
=====				
WATER BUDGET OF THE WHOLE MODEL DOMAIN:				
=====				
FLOW TERM	IN	OUT	IN-OUT	
STORAGE	9.2656250E+06	9.2814450E+06	-1.5820000E+04	
CONSTANT HEAD	1.3663481E+04	2.2801957E+04	-9.1384756E+03	
WELLS	6.6540000E+03	0.0000000E+00	6.6540000E+03	
DRAINS	0.0000000E+00	0.0000000E+00	0.0000000E+00	
RECHARGE	1.8650115E+04	0.0000000E+00	1.8650115E+04	
ET	0.0000000E+00	1.6305080E-03	-1.6305080E-03	
RIVER LEAKAGE	1.9798229E-02	1.2732393E+02	-1.2730413E+02	
HEAD DEP BOUNDS	0.0000000E+00	0.0000000E+00	0.0000000E+00	
STREAM LEAKAGE	0.0000000E+00	0.0000000E+00	0.0000000E+00	
INTERBED STORAGE	0.0000000E+00	0.0000000E+00	0.0000000E+00	
RESERV. LEAKAGE	0.0000000E+00	0.0000000E+00	0.0000000E+00	
SUM	9.3045930E+06	9.3043740E+06	2.1833389E+02	
DISCREPANCY [%]	0.00			

TIME STEP 1 OF STRESS PERIOD 3				
=====				
WATER BUDGET OF THE WHOLE MODEL DOMAIN:				
=====				
FLOW TERM	IN	OUT	IN-OUT	
STORAGE	7.9652440E+06	7.9822605E+06	-1.7016500E+04	
CONSTANT HEAD	1.3651878E+04	2.2610680E+04	-8.9588018E+03	
WELLS	7.6560000E+03	0.0000000E+00	7.6560000E+03	
DRAINS	0.0000000E+00	0.0000000E+00	0.0000000E+00	
RECHARGE	1.8650115E+04	0.0000000E+00	1.8650115E+04	
ET	0.0000000E+00	2.7971654E-03	-2.7971654E-03	
RIVER LEAKAGE	1.9798229E-02	1.2731837E+02	-1.2729857E+02	
HEAD DEP BOUNDS	0.0000000E+00	0.0000000E+00	0.0000000E+00	
STREAM LEAKAGE	0.0000000E+00	0.0000000E+00	0.0000000E+00	
INTERBED STORAGE	0.0000000E+00	0.0000000E+00	0.0000000E+00	
RESERV. LEAKAGE	0.0000000E+00	0.0000000E+00	0.0000000E+00	
SUM	8.0052020E+06	8.0049985E+06	2.0351212E+02	
DISCREPANCY [%]	0.00			

TIME STEP 1 OF STRESS PERIOD 4			
=====			
WATER BUDGET OF THE WHOLE MODEL DOMAIN:			
=====			
FLOW TERM	IN	OUT	IN-OUT
STORAGE	7.2329590E+06	7.2499095E+06	-1.6950500E+04
CONSTANT HEAD	1.3649385E+04	2.2435729E+04	-8.7863438E+03
WELLS	7.4100000E+03	0.0000000E+00	7.4100000E+03
DRAINS	0.0000000E+00	0.0000000E+00	0.0000000E+00
RECHARGE	1.8650115E+04	0.0000000E+00	1.8650115E+04
ET	0.0000000E+00	3.1758659E-03	-3.1758659E-03
RIVER LEAKAGE	1.9798229E-02	1.2731292E+02	-1.2729312E+02
HEAD DEP BOUNDS	0.0000000E+00	0.0000000E+00	0.0000000E+00
STREAM LEAKAGE	0.0000000E+00	0.0000000E+00	0.0000000E+00
INTERBED STORAGE	0.0000000E+00	0.0000000E+00	0.0000000E+00
RESERV. LEAKAGE	0.0000000E+00	0.0000000E+00	0.0000000E+00
SUM	7.2726685E+06	7.2724725E+06	1.9597519E+02
DISCREPANCY [%]	0.00		

TIME STEP 1 OF STRESS PERIOD 5			
=====			
WATER BUDGET OF THE WHOLE MODEL DOMAIN:			
=====			
FLOW TERM	IN	OUT	IN-OUT
STORAGE	6.7403810E+06	6.8048135E+06	-6.4432500E+04
CONSTANT HEAD	1.3653513E+04	2.2275963E+04	-8.6224502E+03
WELLS	8.1430000E+03	0.0000000E+00	8.1430000E+03
DRAINS	0.0000000E+00	0.0000000E+00	0.0000000E+00
RECHARGE	6.4688246E+04	0.0000000E+00	6.4688246E+04
ET	0.0000000E+00	3.5826876E-03	-3.5826876E-03
RIVER LEAKAGE	1.9798229E-02	2.2378432E+02	-2.2376453E+02
HEAD DEP BOUNDS	0.0000000E+00	0.0000000E+00	0.0000000E+00
STREAM LEAKAGE	0.0000000E+00	0.0000000E+00	0.0000000E+00
INTERBED STORAGE	0.0000000E+00	0.0000000E+00	0.0000000E+00
RESERV. LEAKAGE	0.0000000E+00	0.0000000E+00	0.0000000E+00
SUM	6.8268660E+06	6.8273135E+06	-4.4747220E+02
DISCREPANCY [%]	-0.01		

TIME STEP 1 OF STRESS PERIOD 6			
=====			
WATER BUDGET OF THE WHOLE MODEL DOMAIN:			
=====			
FLOW TERM	IN	OUT	IN-OUT
STORAGE	6.3800645E+06	6.4513725E+06	-7.1308000E+04
CONSTANT HEAD	1.3662915E+04	2.2129318E+04	-8.4664033E+03
WELLS	8.2510000E+03	0.0000000E+00	8.2510000E+03
DRAINS	0.0000000E+00	0.0000000E+00	0.0000000E+00
RECHARGE	7.1344156E+04	0.0000000E+00	7.1344156E+04
ET	0.0000000E+00	3.7442499E-03	-3.7442499E-03
RIVER LEAKAGE	1.9798229E-02	1.2730275E+02	-1.2728295E+02
HEAD DEP BOUNDS	0.0000000E+00	0.0000000E+00	0.0000000E+00
STREAM LEAKAGE	0.0000000E+00	0.0000000E+00	0.0000000E+00
INTERBED STORAGE	0.0000000E+00	0.0000000E+00	0.0000000E+00
RESERV. LEAKAGE	0.0000000E+00	0.0000000E+00	0.0000000E+00
SUM	6.4733225E+06	6.4736290E+06	-3.0653375E+02
DISCREPANCY [%]	0.00		

TIME STEP 1 OF STRESS PERIOD 7			
=====			
WATER BUDGET OF THE WHOLE MODEL DOMAIN:			
=====			
FLOW TERM	IN	OUT	IN-OUT
STORAGE	6.0017495E+06	6.2758805E+06	-2.7413100E+05
CONSTANT HEAD	1.3669018E+04	2.1993643E+04	-8.3246250E+03
WELLS	8.3050000E+03	0.0000000E+00	8.3050000E+03
DRAINS	0.0000000E+00	0.0000000E+00	0.0000000E+00
RECHARGE	2.7436531E+05	0.0000000E+00	2.7436531E+05
ET	0.0000000E+00	4.1582370E-03	-4.1582370E-03
RIVER LEAKAGE	1.9798229E-02	1.2729802E+02	-1.2727822E+02
HEAD DEP BOUNDS	0.0000000E+00	0.0000000E+00	0.0000000E+00
STREAM LEAKAGE	0.0000000E+00	0.0000000E+00	0.0000000E+00
INTERBED STORAGE	0.0000000E+00	0.0000000E+00	0.0000000E+00
RESERV. LEAKAGE	0.0000000E+00	0.0000000E+00	0.0000000E+00
SUM	6.2980890E+06	6.2980015E+06	8.7405121E+01
DISCREPANCY [%]	0.00		

TIME STEP 1 OF STRESS PERIOD 8			
=====			
WATER BUDGET OF THE WHOLE MODEL DOMAIN:			
=====			
FLOW TERM	IN	OUT	IN-OUT
STORAGE	5.7243470E+06	6.0288020E+06	-3.0445500E+05
CONSTANT HEAD	1.3677438E+04	2.1867975E+04	-8.1905361E+03
WELLS	8.3590000E+03	0.0000000E+00	8.3590000E+03
DRAINS	0.0000000E+00	0.0000000E+00	0.0000000E+00
RECHARGE	3.0397831E+05	0.0000000E+00	3.0397831E+05
ET	0.0000000E+00	4.3941019E-03	-4.3941019E-03
RIVER LEAKAGE	1.9531537E-02	1.2729332E+02	-1.2727379E+02
HEAD DEP BOUNDS	0.0000000E+00	0.0000000E+00	0.0000000E+00
STREAM LEAKAGE	0.0000000E+00	0.0000000E+00	0.0000000E+00
INTERBED STORAGE	0.0000000E+00	0.0000000E+00	0.0000000E+00
RESERV. LEAKAGE	0.0000000E+00	0.0000000E+00	0.0000000E+00
SUM	6.0503620E+06	6.0507975E+06	-4.3550180E+02
DISCREPANCY [%]	-0.01		

TIME STEP 1 OF STRESS PERIOD 9			
=====			
WATER BUDGET OF THE WHOLE MODEL DOMAIN:			
=====			
FLOW TERM	IN	OUT	IN-OUT
STORAGE	5.4647025E+06	5.7790965E+06	-3.1439400E+05
CONSTANT HEAD	1.3690022E+04	2.1756760E+04	-8.0667373E+03
WELLS	8.6340000E+03	0.0000000E+00	8.6340000E+03
DRAINS	0.0000000E+00	0.0000000E+00	0.0000000E+00
RECHARGE	3.1467941E+05	0.0000000E+00	3.1467941E+05
ET	0.0000000E+00	4.5928704E-03	-4.5928704E-03
RIVER LEAKAGE	1.9347789E-02	1.2728933E+02	-1.2726998E+02
HEAD DEP BOUNDS	0.0000000E+00	0.0000000E+00	0.0000000E+00
STREAM LEAKAGE	0.0000000E+00	0.0000000E+00	0.0000000E+00
INTERBED STORAGE	0.0000000E+00	0.0000000E+00	0.0000000E+00
RESERV. LEAKAGE	0.0000000E+00	0.0000000E+00	0.0000000E+00
SUM	5.8017060E+06	5.8009805E+06	7.2539435E+02
DISCREPANCY [%]	0.01		

TIME STEP 1 OF STRESS PERIOD 10

=====

WATER BUDGET OF THE WHOLE MODEL DOMAIN:

=====

FLOW TERM	IN	OUT	IN-OUT
STORAGE	5.2804655E+06	5.5174285E+06	-2.3696300E+05
CONSTANT HEAD	1.3712961E+04	2.1647766E+04	-7.9348047E+03
WELLS	6.9960000E+03	0.0000000E+00	6.9960000E+03
DRAINS	0.0000000E+00	0.0000000E+00	0.0000000E+00
RECHARGE	2.3781014E+05	0.0000000E+00	2.3781014E+05
ET	0.0000000E+00	4.8415642E-03	-4.8415642E-03
RIVER LEAKAGE	1.9347789E-02	1.2728544E+02	-1.2726609E+02
HEAD DEP BOUNDS	0.0000000E+00	0.0000000E+00	0.0000000E+00
STREAM LEAKAGE	0.0000000E+00	0.0000000E+00	0.0000000E+00
INTERBED STORAGE	0.0000000E+00	0.0000000E+00	0.0000000E+00
RESERV. LEAKAGE	0.0000000E+00	0.0000000E+00	0.0000000E+00
SUM	5.5389845E+06	5.5392035E+06	-2.1893500E+02
DISCREPANCY [%]	0.00		

TIME STEP 1 OF STRESS PERIOD 11

=====

WATER BUDGET OF THE WHOLE MODEL DOMAIN:

=====

FLOW TERM	IN	OUT	IN-OUT
STORAGE	5.1566915E+06	5.1616625E+06	-4.9710000E+03
CONSTANT HEAD	1.3737761E+04	2.1542385E+04	-7.8046240E+03
WELLS	7.4460000E+03	0.0000000E+00	7.4460000E+03
DRAINS	0.0000000E+00	0.0000000E+00	0.0000000E+00
RECHARGE	6.9362144E+03	0.0000000E+00	6.9362144E+03
ET	0.0000000E+00	5.0473064E-03	-5.0473064E-03
RIVER LEAKAGE	1.9347789E-02	1.2728144E+02	-1.2726209E+02
HEAD DEP BOUNDS	0.0000000E+00	0.0000000E+00	0.0000000E+00
STREAM LEAKAGE	0.0000000E+00	0.0000000E+00	0.0000000E+00
INTERBED STORAGE	0.0000000E+00	0.0000000E+00	0.0000000E+00
RESERV. LEAKAGE	0.0000000E+00	0.0000000E+00	0.0000000E+00
SUM	5.1848115E+06	5.1833320E+06	1.4793232E+03
DISCREPANCY [%]	0.03		

TIME STEP 1 OF STRESS PERIOD 12

=====

WATER BUDGET OF THE WHOLE MODEL DOMAIN:

=====

FLOW TERM	IN	OUT	IN-OUT
STORAGE	4.9660005E+06	4.9656440E+06	3.5650000E+02
CONSTANT HEAD	1.3762852E+04	2.1442178E+04	-7.6793262E+03
WELLS	7.4460000E+03	0.0000000E+00	7.4460000E+03
DRAINS	0.0000000E+00	0.0000000E+00	0.0000000E+00
RECHARGE	0.0000000E+00	0.0000000E+00	0.0000000E+00
ET	0.0000000E+00	5.2425275E-03	-5.2425275E-03
RIVER LEAKAGE	1.9347789E-02	1.2727766E+02	-1.2725832E+02
HEAD DEP BOUNDS	0.0000000E+00	0.0000000E+00	0.0000000E+00
STREAM LEAKAGE	0.0000000E+00	0.0000000E+00	0.0000000E+00
INTERBED STORAGE	0.0000000E+00	0.0000000E+00	0.0000000E+00
RESERV. LEAKAGE	0.0000000E+00	0.0000000E+00	0.0000000E+00
SUM	4.9872095E+06	4.9872135E+06	-4.0897307E+00
DISCREPANCY [%]	0.00		